FB100 Plasma Chemical Processes

Mgr. Ondřej Jašek, Ph.D.
jasek@physics.muni.cz

Fullerene synthesis

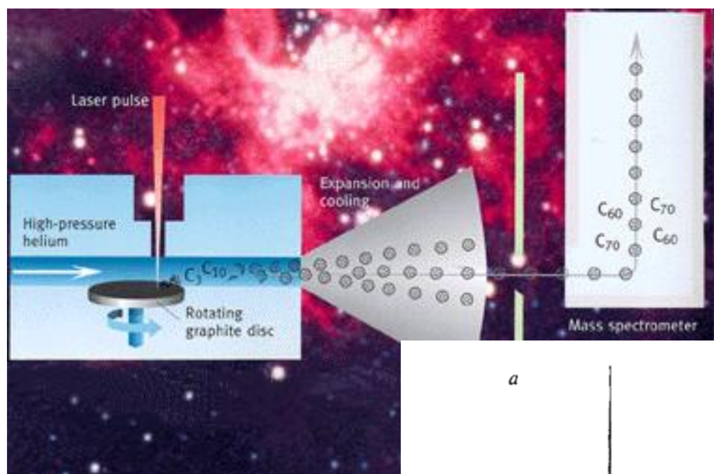

Laser ablation of graphite target in He atmosphere pressure ~ 100 Torr (13 kPa)
Separation in centrifuge and liquid chromatography
Fast detection by color in fullerene/toluene suspension C_{60} – wine red, C_{70} brown.

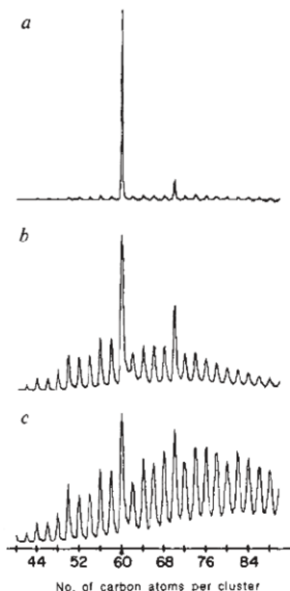

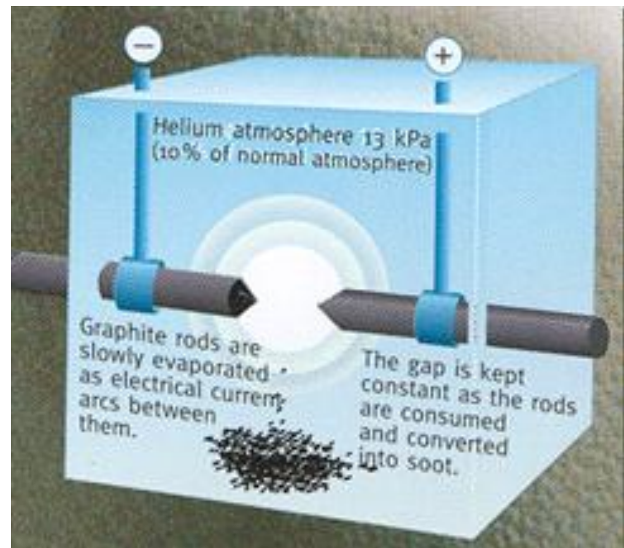

Arc discharge
He atmosphere, 13 kPa,
Arc discharge electric parameters: ~100 A, 24V.
Deposit collected on reactors cooled reactor walls
Analysis – mass spectrometry
C_{60}-720 amu, C_{70} – 840 amu.
NMR C_{60} 1 line, C_{70} 5 lines - symmetries.

Lawrence T. Scott, Methods for the Chemical Synthesis of Fullerenes, Angew. Chem. Int. Ed. 2004, 43, 4994 – 5007.

Fullerene synthesis

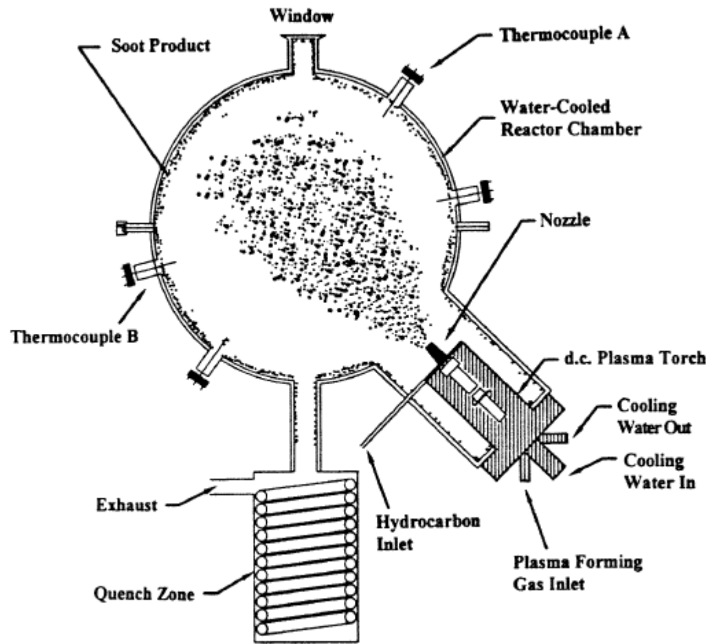

Figure 1. Set-up of fullerene synthesis reactor.

Table 1. Experimental conditions for fullerene soot production.

Torch power (kW)	55, 65
Helium flow rate (slpm)	225
C_2Cl_4 feed rate (mol/min)	0.29
He carrier gas flow rate (slpm)	20
Run duration (min)	4

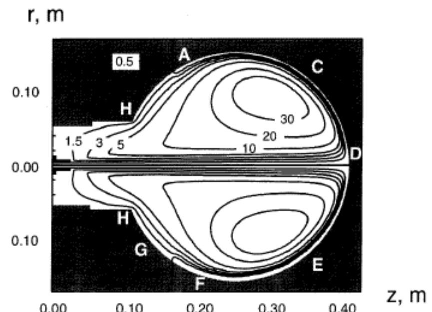

Figure 3. Isocontours of the helium stream function, normalized by the torch flow rate.

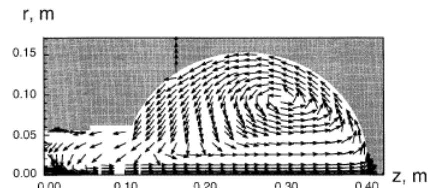

Figure 4. Direction of velocities in the reactor.

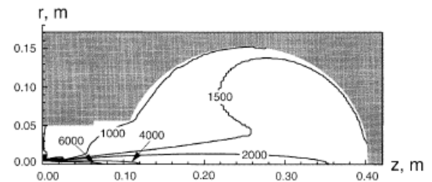

Figure 5. Isocontours of temperature (K).

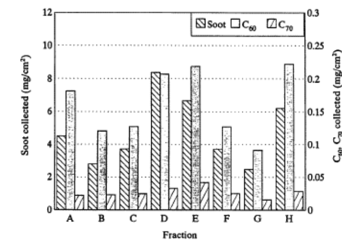

Figure 9. Collection rates of total soot, C_{60} and C_{70}, power = 55 kW.

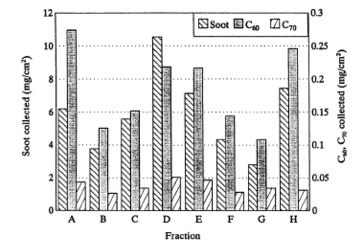

Figure 10. Collection rates of total soot, C_{60} and C_{70}, power = 65 kW.

J.-F. Bilodeauyx, T. Alexakisyz, J.-L. Meuniery and P. G. Tzantrizosz, Model of the synthesis of fullerenes by the plasma torch dissociation of C2Cl4, J. Phys. D: Appl. Phys. 30 (1997) 2403–2410.

Fullerene synthesis by decompostion of CCl4 in rf dicharge in helium atmosphere

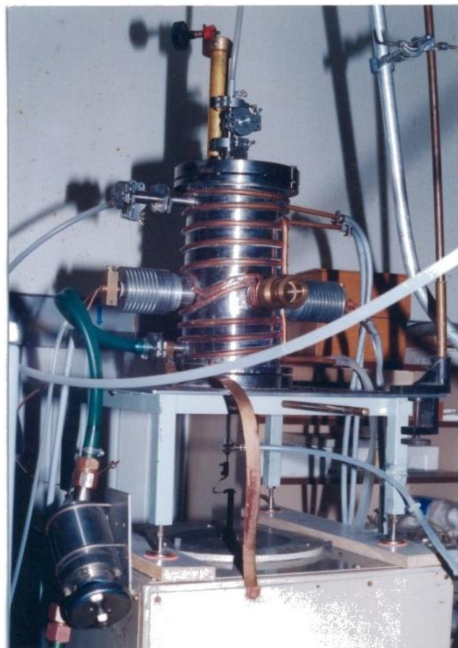

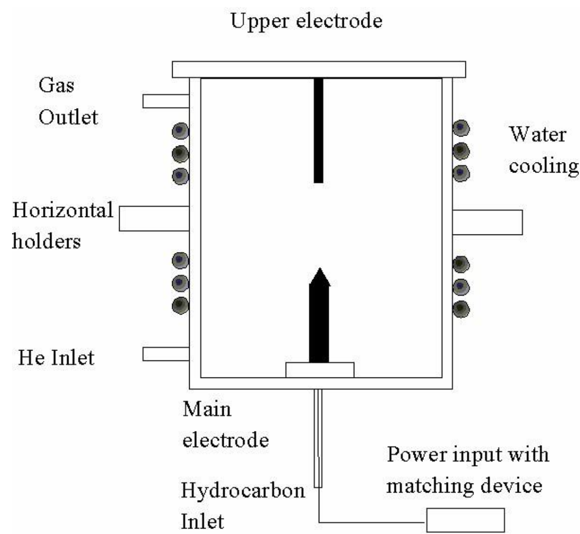

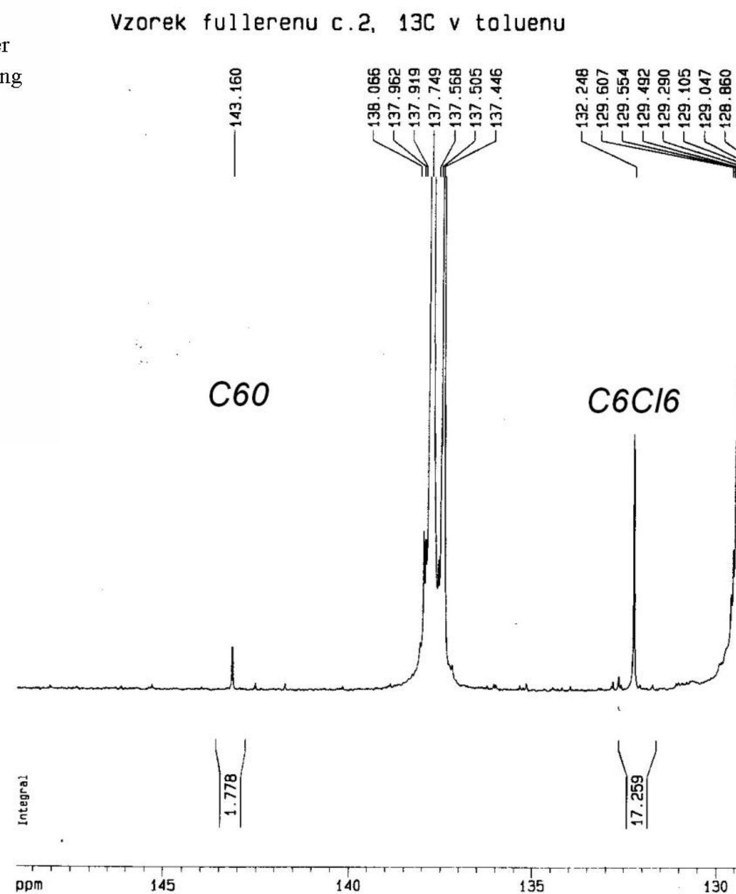

Stainless steele water cooled reactor 20 cm diameter
25 cm height
Precursors toluene, benzene, CCl_4 (0,2 – 0,3 cm^3/min)
RF power - 27 MHz,2 kW, dep. time 10 -30 minut
Helium atmosphere 60 – 150 Torr

Growth of diamond layers – ultrananocrystalline diamond

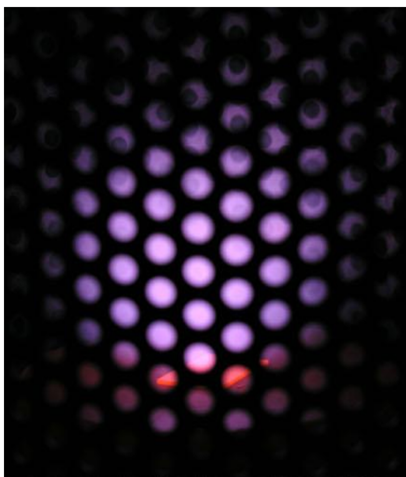

- microwave power (2.45 GHz) 900–950 W
- pressure 7.5 kPa
- substrate temperature 800–950 °C
- CH_4/H_2 gas mixture (2 and 9.4 % of CH_4)
- deposition time 1–40 min
- polished Si, no pretreatment

Nucleation of ultra-nanocrystalline diamond

Bias Enhanced Nucleation – BEN in-situ nucleation density ~ 10^{12} cm^2

- BEN is traditionally used with DC bias and during nucleation phase

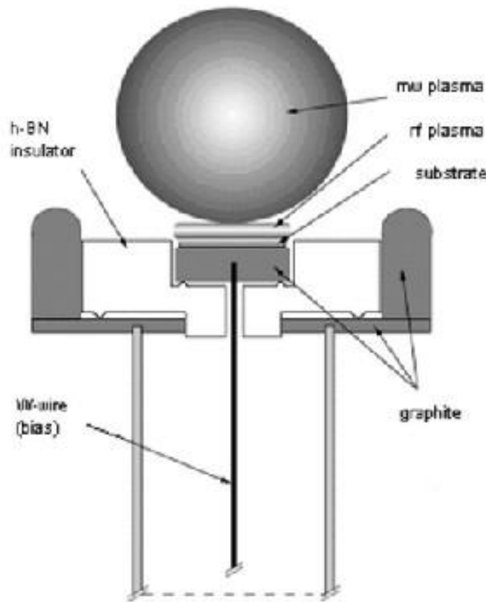

- our approach combined MW (900 W) and RF (35 W) discharges, DC bias was a result of RF sheath properties
- ion bombardment during the deposition phase was necessary for high renucleation rate

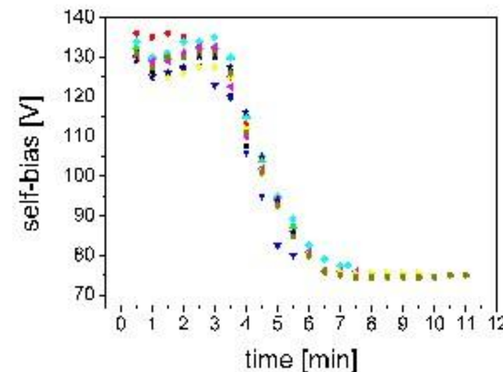

Ultra-nanocrystalline diamond

High concentration of CH_4 – 10 % against 1-2 % traditionally used, 2x lower layer roughness

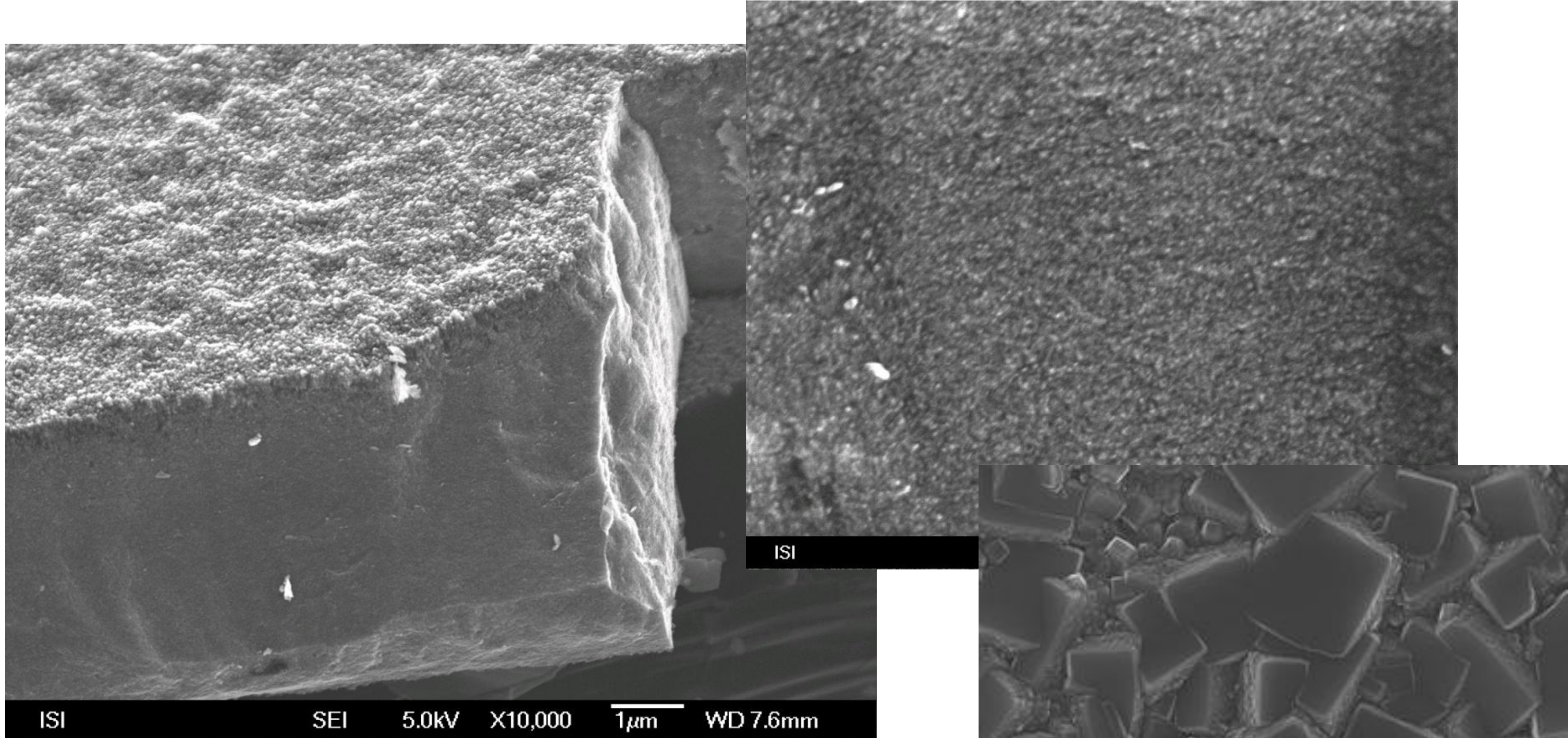

H/N/C mixtures – T. Frgala, PhD Thesis
Preferential growth of <100> orientation

Nucleation of ultra-nanocrystalline diamond

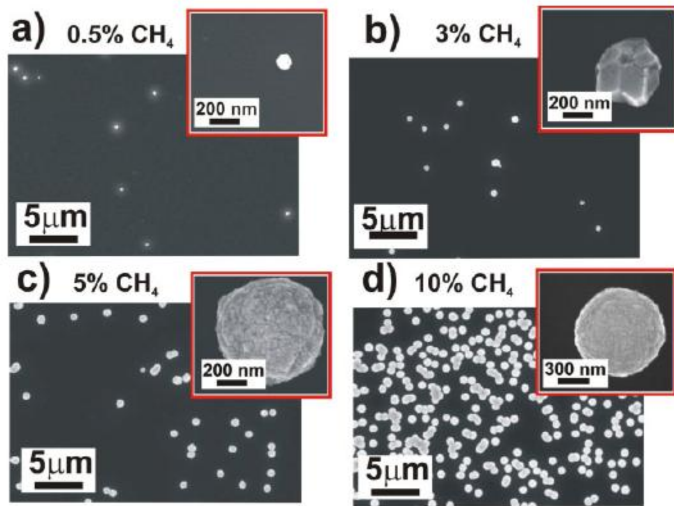

Figure 1 SEM images of the Si substrates nucleated for 1 h in the hot plasma system at different ratios of CH_4 to H_2 (inserted images show details of the diamond cluster morphology).

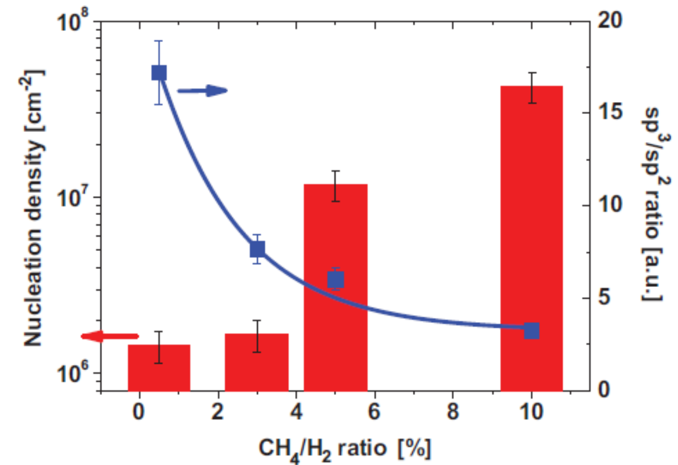

Figure 2 Nucleation densities of the samples nucleated in the hot plasma (red columns) and corresponding diamond (sp^3) to non-diamond (sp^2) ratio (blue curve) calculated from Raman spectra at various methane concentrations.

Astex type reactor MW power 2500 W, pressure 50 mbar, and process time 1 h. Si substrate (10 x 10 mm) is 1-2 cm from plasma ball and is heated by plasma to 750 C.

The diamond can also be nucleated from CO_2/H_2 mixture in the remote mw plasma reactor. The nucleation density is higher and sp^2 content lower but time of nucleation is 15 hours. At high CO_2 concentrations (40 %) the diamond seeds are etched away.

Tibor Izak, Alexey Sveshnikov, Pavel Demo, and Alexander Kromka, Enhanced spontaneous nucleation of diamond nuclei in hot and cold microwave plasma systems, Phys. Status Solidi B 250, No. 12, 2753–2758 (2013).

Low temperature diamond synthesis

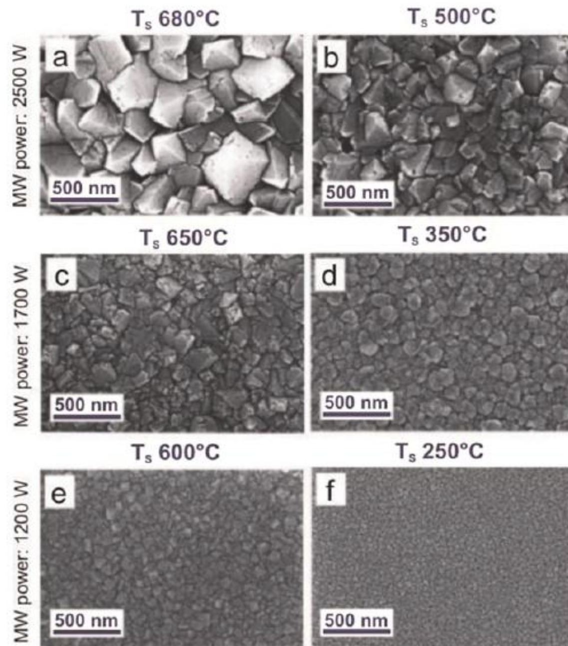

Figure 1 (online colour at: www.pss-b.com) Top-view SEM images of diamond film morphology deposited at different substrate temperatures (T_S); upper row: diamond films deposited at 2500 W, middle row: 1700 W, bottom row: 1200 W of MW power. The right column represents the minimal substrate (or deposition) temperature at corresponding MW power without external ohmic substrate heating.

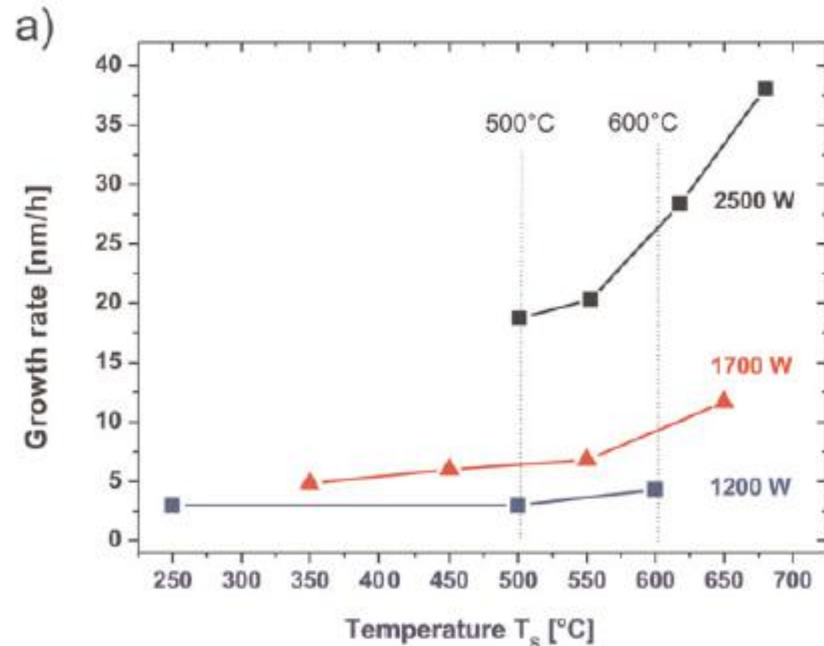

Diamond layer ultrasonically seeded by ultradispersed detonation diamond (UDD) powder on Si (10x10 mm). Pressure 0.1 mbar, deposition time 15 h, gas mixture 2.5% of CH_4 and 10% of CO_2 in H_2. Temperature regulated by plasma power and table heater.

Tibor Izak, Oleg Babchenko, Marian Varga, Stepan Potocky and Alexander Kromka, Low temperature diamond growth by linear antenna plasma CVD over large area, Phys. Status Solidi B 249, No. 12, 2600–2603 (2012).

Carbon nanotubes synthesis

High temperature methods

-Arc discharge between grapthite electrodes

-*Graphite target laser ablation*

-*high temperature (3500 °C), short growth time ms, SWCNTs require catalyst – transition metal (Fe,Ni,Co,Mo), carbon diffuses into catalytic particle and precipitates out in the form of nanotube, several nanotubes can growth from one particle*

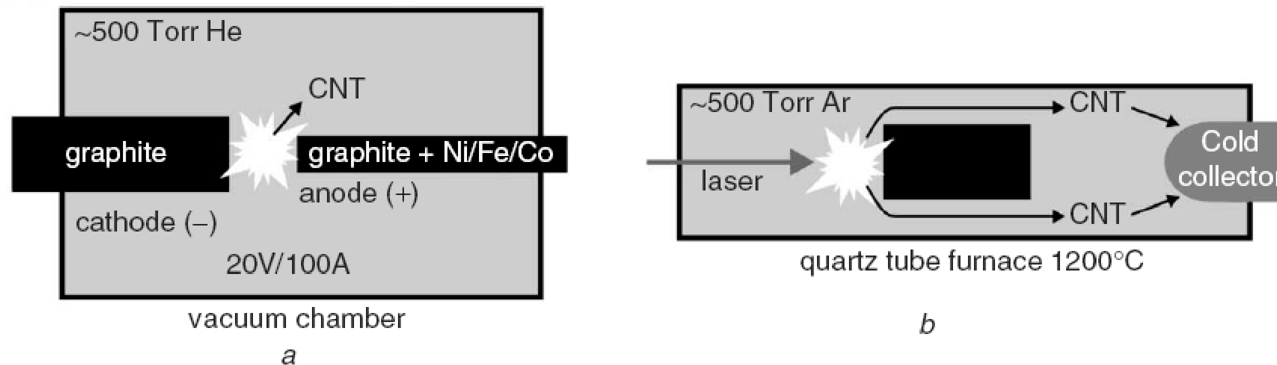

K.B.K. Teo, R.G. Lacerda et al.. "*Carbon Nanotube Technology for Solid State and Vacuum Electronics*" IEE Proceedings in Circuits, Devices and Systems (Nanoelectronics issue) **151**, 443 (2004).

Carbon nanostructures synthesis

Low temperature methods *– thermal CVD, PECVD (rf, mw, dc, hf)*
hydrocarbon decomposition in presence of catalyst
Temperature 500-1200 °C, longer deposition times- minutes even hours, transition metal catalyst plays significant role and serves as template for nanotube growth
PECVD *– lowering deposition temperature, compatibility with microelectronics industry, electric field vertical alignment (0.15 V/μm)*

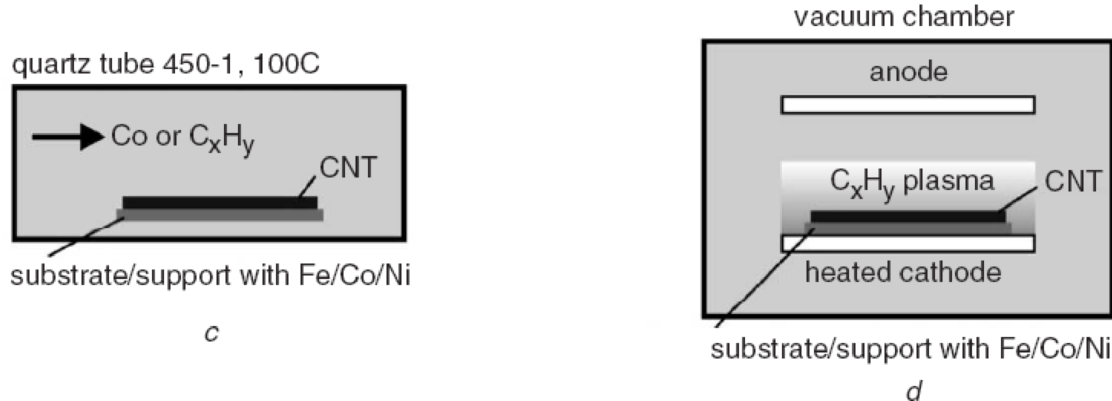

M. Meyyappan, L. Delzeit, A. Cassell, D. Hash. *Plasma Sources Sci. Technol*. **12**, 205 (2003), M. Meyyappan, J. Phys. D: Appl. Phys. **42** (2009) 213001

Catalyst in PECVD

- *Transition metal catalyst – Fe,Co,Mo,Ni or combination - finite solubility in C leads to CNTs growth by diffusion, saturation and precipitation mechanism*
- *Catalyst must be in the form of particles, particles and their surface atoms have high mobility in nm scale even if the metal is in solid state and can behave like liquid*
- *in lower temperature surface diffusion dominates, in higher volume diffusion*
- *Support catalyst (evaporation, sputtering, wet catalyst, colloids etc.) or floating catalyst – decomposition of organometallics*
- *Catalyst poisoning effect – covering the particle with amorphous carbon*

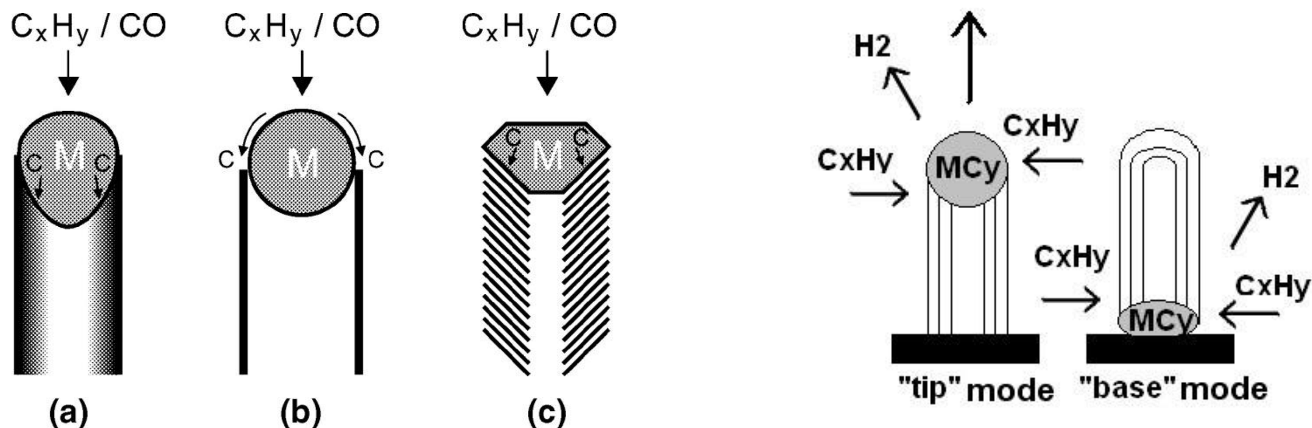

K. B.K. Teo, C. Singh, M. Chhowalla, W. I. Milne, Encyclopedia of Nanoscience and Nanotechnology, Vol. 10, Eds. H.S. Nalwa, American Scientific Publishers, Los Angeles, 2003

CNTs growth in PECVD systems

DC glow discharge resistively heated carbon electrode – cathode with the sample (Si/SiO_2 buffer layer and Ni catalyst 0.5-20 nm) Anode (2 mm diameter by 1 cm length copper wire) was 2 cm from cathode. Sample heated to 750 C under H_2 and held at this temperature for 15 minutes after that 200 sccm of NH_3 was introduced to pressure of 465 Pa. The deposition was carried out in mixture of C_2H_2 and NH_3 for 15 minutes.

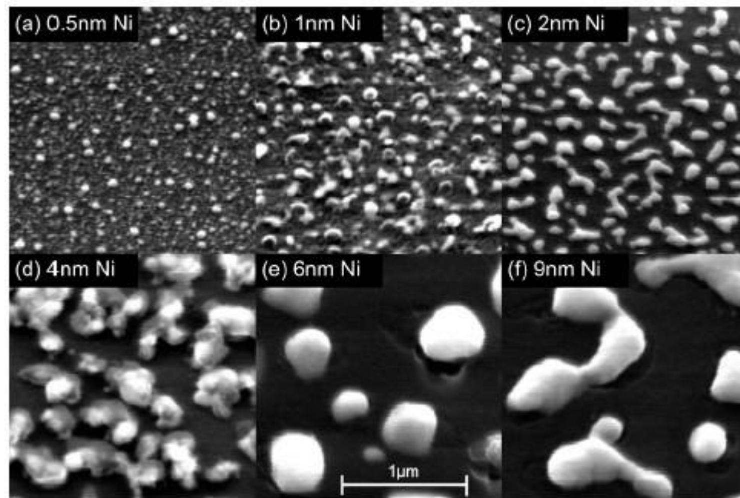

FIG. 1. SEM photographs of Ni films with varying thicknesses deposited using magnetron sputtering on 50 nm of ECR SiO_2 after annealing at 750 °C in 20 Torr of H_2 for 15 min.

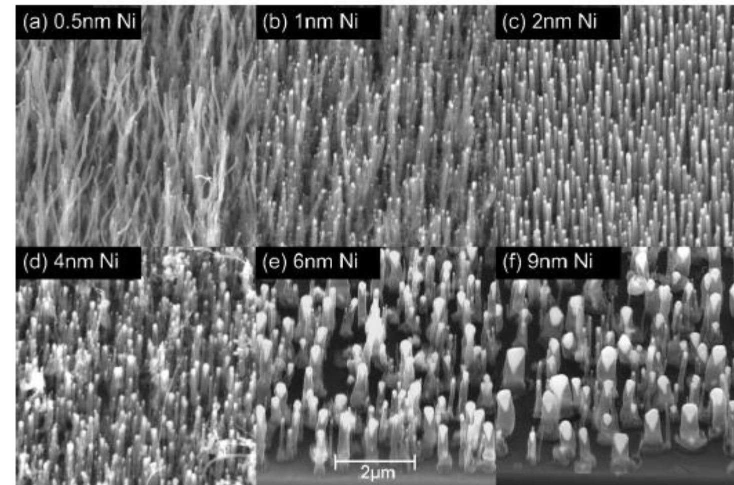

FIG. 4. SEM photographs of nanotubes grown on Ni layers of various initial thicknesses shown in Fig. 1. Standard growth conditions (bias voltage = −600V, C_2H_2:NH_3=75:200, time=15 min) were used for all depositions.

Chhowalla et al., Growth process conditions of vertically aligned carbon nanotubes using plasma enhanced chemical vapor depositionJ. Appl. Phys., Vol. 90, No. 10, 2001,5308

CNTs growth in PECVD systems

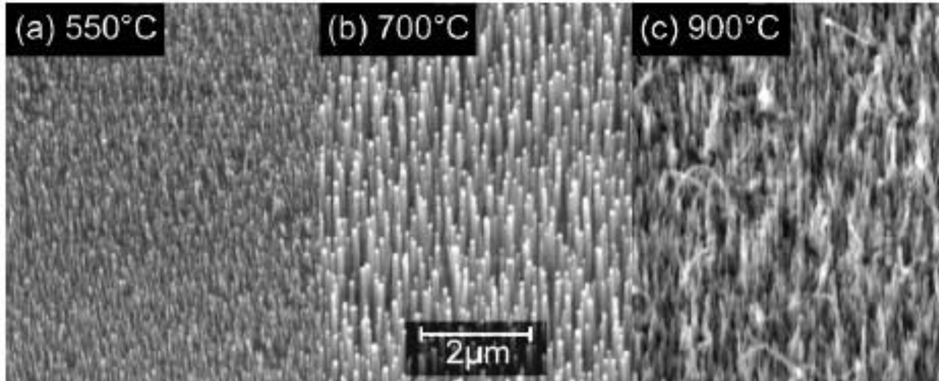

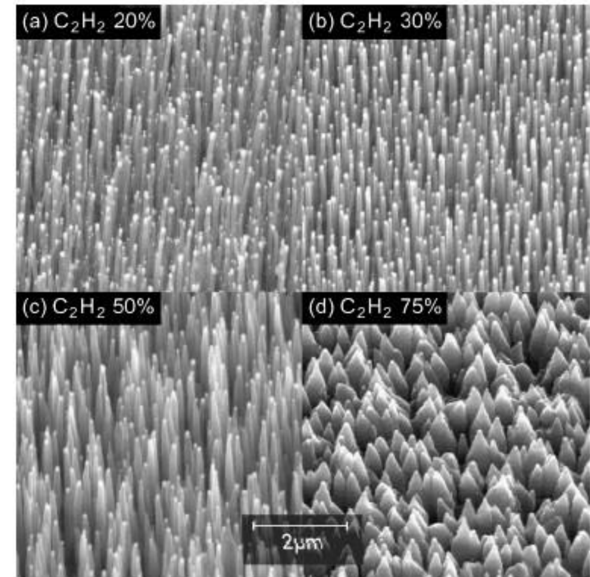

NH_3 flow at 100 sccm

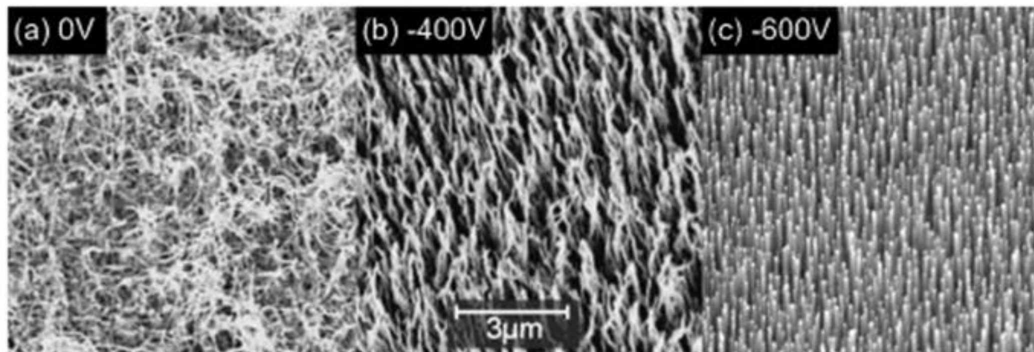

2 nm Ni catalyst

CNTs growth in PECVD systems

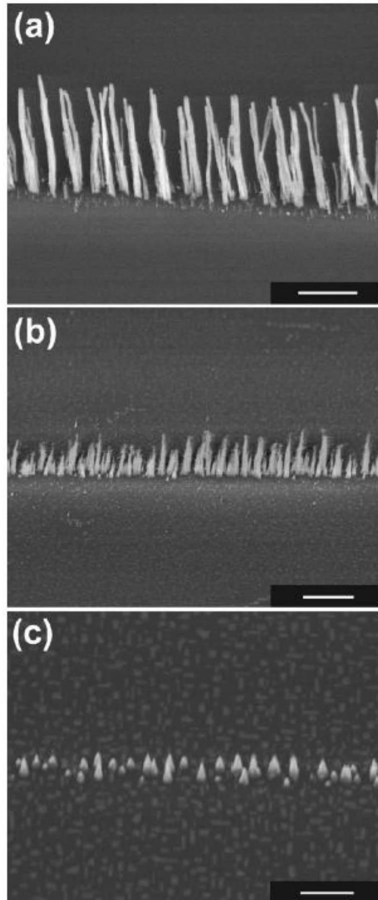

FIG. 2. SEM photographs of vertically aligned CNFs grown from e-beam patterned Ni lines at (a) 500 °C, (b) 270 °C, and (c) 120 °C. A tilt angle of 40° was used for imaging [scale bars: (a) and (b) 1 μm and (c) 500 nm].

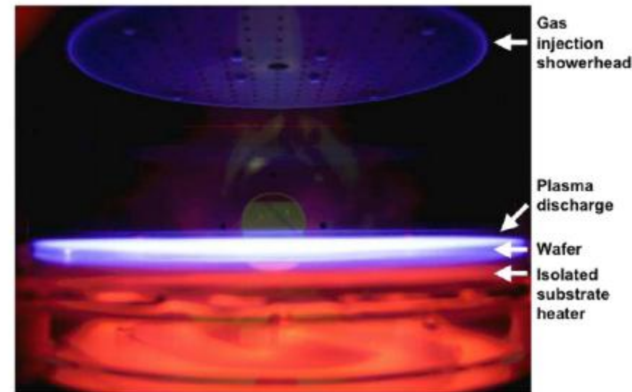

Figure 4. Wafer scale PECVD reactor. (Image courtesy of K B K Teo.)

DC discharge between the heater stage (cathode) and the gas shower head (anode), 2 cm above the stage was ignited by applying a fixed voltage of 600 V.

$Si/SiO_2/Ni$ (6 nm) substrate

Samples annealed in 120 Pa NH_3 for 15 minutes. Deposition carried out in $C_2H_2:NH_3$ 50:200 sccm at 150 Pa for 30 minutes.

S. Hofmann, C. Ducati, and J. Robertson, B. Kleinsorge, Low-temperature growth of carbon nanotubes by plasma-enhanced chemical vapor deposition, Appl. Phys. Lett., Vol. 83, No. 1, 135.

CNTs growth in PECVD systems

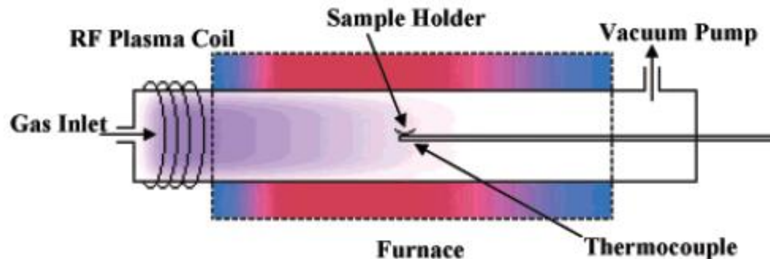

Figure 1. Schematic drawing of the PECVD reactor used for the synthesis of SWNTs.

RF (13.56 MHz) capactive coupled discharge with 4 inch quartz tube. Sample Si/SiO_2/Fe Ferritin or 0.1 nm Fe by electron beam evaporation of Fe 40 cm from the coil in the furnace. Sample annealed in in Ar to 600 °C and then 60 sccm Ar/CH4 (80%) at 67 Pa. Plasma was turned on for 3 minutes with 75 W power.

No CNTs without the plasma.

Y. Li et .al. , Preferential Growth of Semiconducting Single-Walled Carbon Nanotubes by a Plasma Enhanced CVD Method, Nano Lett., Vol. 4, No. 2, 2004, 317.

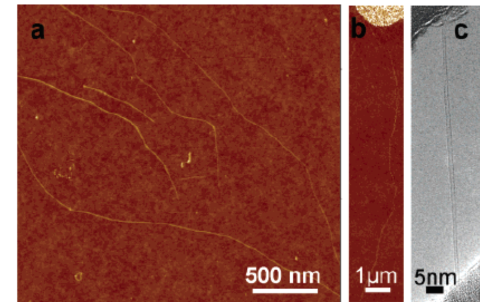

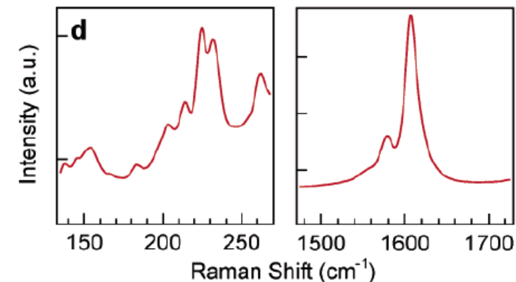

Figure 2. SWNTs grown at 600 °C. (a) AFM image of nanotubes grown from low-density ferritin deposition on a SiO_2 substrate. (b) AFM image of a tube grown from an iron-film island (nominal thickness 1 Å). (c) TEM image of an as-grown SWNT (diameter = 1.2 nm). (d) Left panel: Raman data for the RBMs of SWNTs grown by PECVD. Right panel: The G-band of SWNT vibration (clear peaks at 1578 and 1608 cm^{-1}, due to splitting of the in-plane graphene mode at 1580 cm^{-1} from graphene to tubes). Raman data here was obtained with a SWNT mat grown on a uniform Fe film deposited on SiO_2, and the data were sum of 75 spectra recorded over the sample.

Table 1. Summary of the Diameter Distributions and Percentages of s- and m-SWNTs Grown by PECVD (with several batches of devices) and HiPco

	measured Raman RBM (cm^{-1})	diameter range (from Raman)	total # of devices	total # of Tubes (N_T)	# of s-SWNTs (N_s)	# of m-SWNTs	s-SWNT % = (p)
PECVD	161−284	0.8 nm−1.5 nm	375	701	626	75	89.3 ± 2.3%
HiPco	201−264	0.8 nm−1.3 nm	80	164	100	64	61.0 ± 7.6%

Possible negative influence of plasma in PECVD

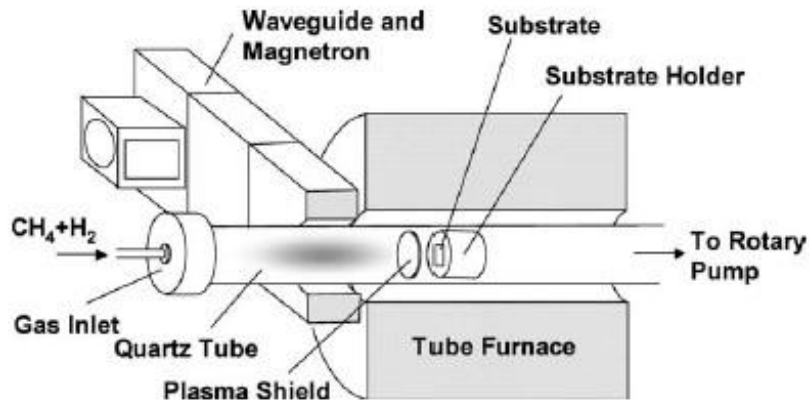

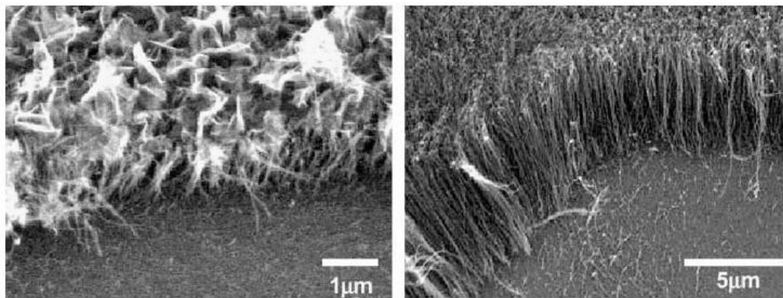

Kinoshita H. et.al., Carbon 42 (2004) 2735

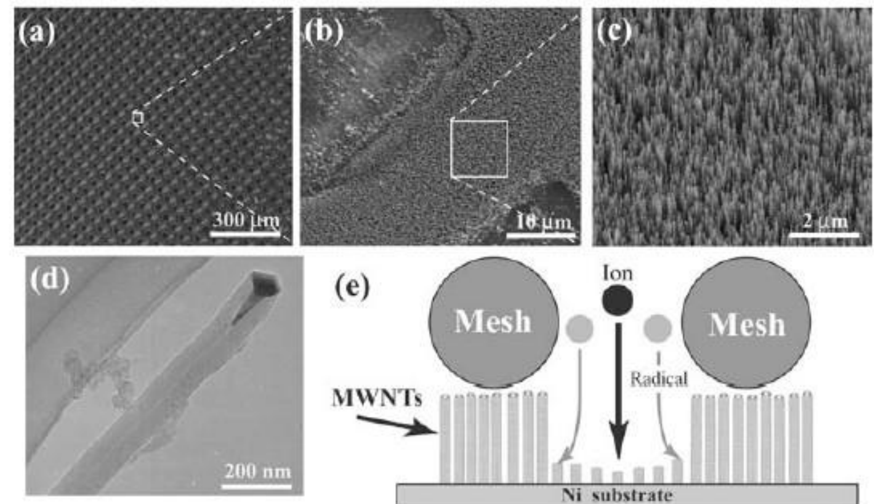

Jeong et al., Appl. Phys. A 79, 85 (2004)

PECVD at atmospheric pressure

- Plasma enhanced chemical vapor deposition with various sources
- Operation at 100 kPa without a vacuum system
- Plasma arcs, jets and torches – mostly operated in floating catalyst regime, most often used with microwave sources
- Atmospheric pressure glow discharge (APGD) diffusion form of dielectric barrier discharge (DBD) – deposition on substrates with heated electrode

Atmospheric pressure glow discharge

- Discharge configuration when one or both electrodes are covered with dielectric barrier (used for ozone production since 19th century)
- Filamentary DBD can be made diffusive with addition of He or Ne,which are both expensive gases, in can be also made homogeneous in Ar with certain hydrocarbons, N_2 or ammonia addition or special electrode structure.
- It was shown that during the current increase the discharge transits from a non-self-sustained discharge to a Townsend discharge and then to a subnormal glow discharge in He and Ar/NH3 and, therefore, can be called atmospheric pressure glow discharge (APGD).
- APGD has only 1 broad current pulse in each half period while DBD has many nanosecond current pulses, non-thermal plasma at atmospheric pressure

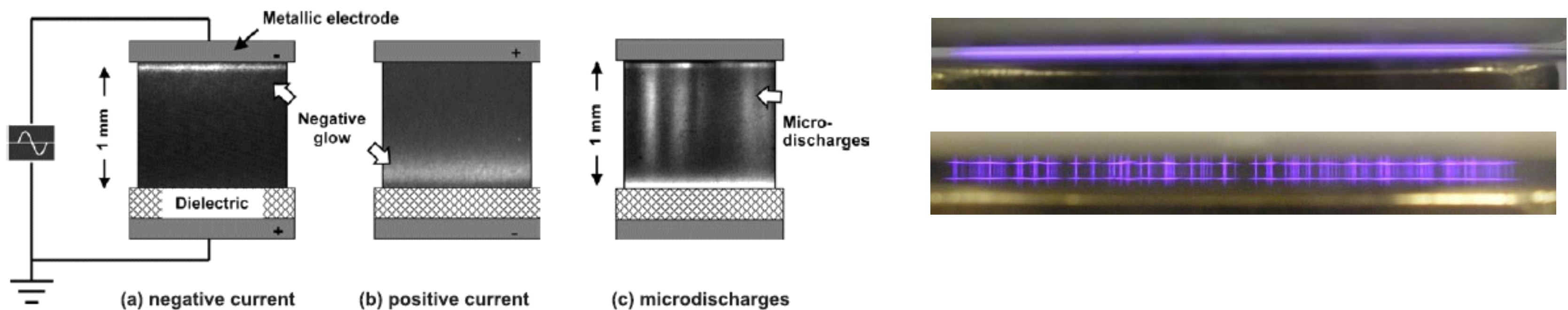

T. Nozaki, Y. Kimura and K. Okazaki, J. Phys. D: Appl. Phys. 35 (2002) 2779–2784

CNTs growth in APGD

First CNTs growth published by T. Nozaki, Y. Kimura and K. Okazaki,
J. Phys. D: Appl. Phys. 35 (2002) 2779–2784
Quartz substrate with 20 nm metal plated Ni, pretreatment in H_2 for 30 min at 600 °C
Operation in kHz mode resulted in deposition of many defective structures

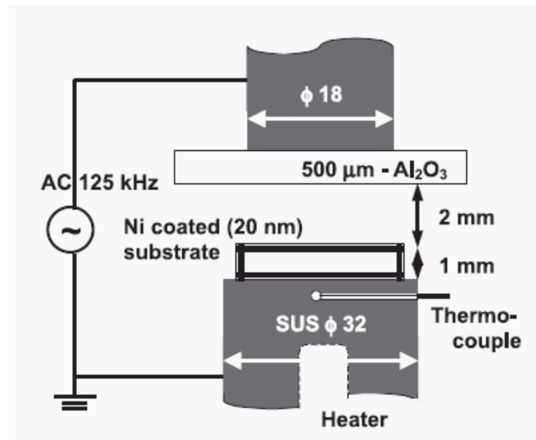

Figure 3. Electrode configuration.

Table 1. Growth parameters.

Growth temperature (°C)	400, 500, 600
Growth time (min)	5–30
H_2/CH_4 ration (-)	0, 5, 10
Flow rate of gas mixture (scc min^{-1})	APG: He : H_2 : CH_4 = 900 : 100 : 0–20 DBD: He : H_2 : CH_4 = 150 : 150 : 15
Pressure (Torr)	760
Power (current peak)	~4 W cm^{-2} (~15 mA cm^{-2})

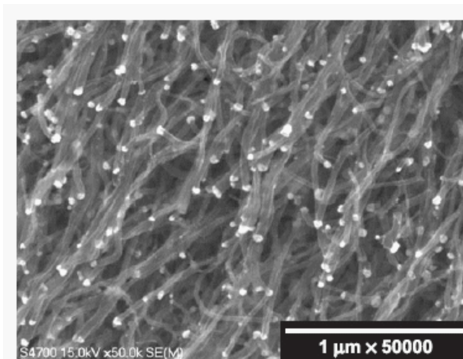

Figure 6. CNTs with uniform diameter of 40–50 nm and number density of 10^9–10^{10} cm^{-2} obtained after 30 min deposition.

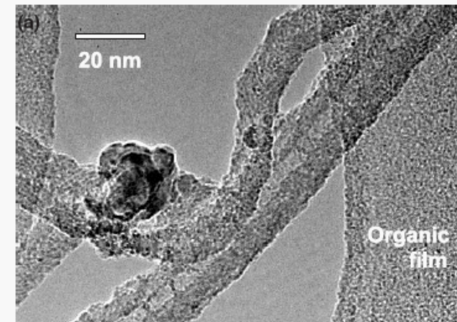

CNTs growth in APGD

- APG was also successfully used with modified electrode (pin to plate) by Y.-H. Lee, S.-H. Kyung, C.-W. Kim, G.-Y. Yeom. Carbon 44, 799 (2006) and capillary type by S.-J. Kyung, Y.-H. Lee, C.-W. Kim, J.-H. Lee, G.-Y. Yeom. Thin Solid Films 506–507, 268 (2006).

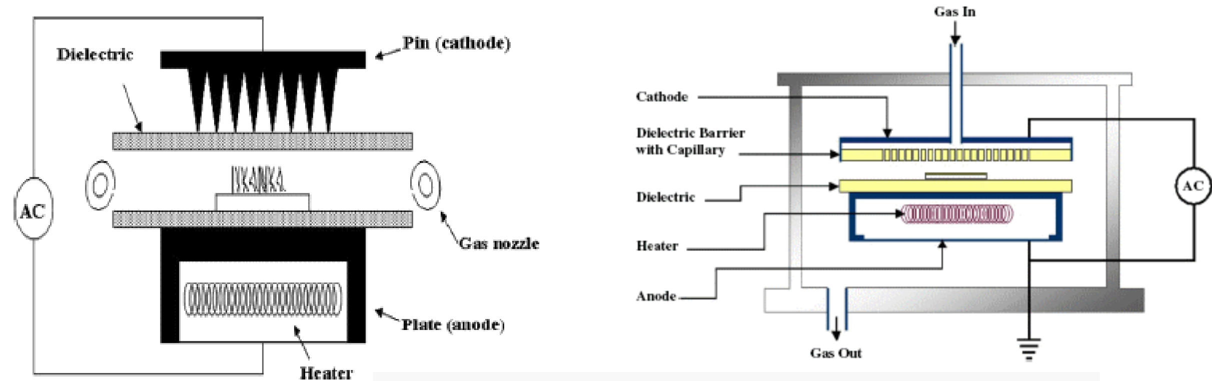

Ni (5 nm)/Cr (100 nm)/Si substrates
He(6 slm)/NH_3(90 sccm) plasma
with pretreatment at 400 °C for 5 min
He/C_2H_2(60 sccm) plasma
He/N_2(60 sccm)/C_2H_2 plasma
He/NH_3/C_2H_2 plasma
He/NH_3/C_2H_2 with dc bias 1.2 kV

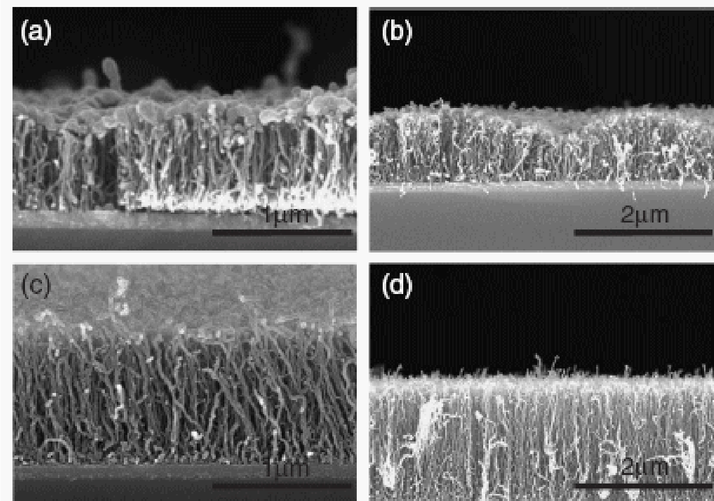

CNTs growth in APGD

- In 2006 T. Nozaki et al. J. Appl.Phys. 99, 024310 used radio-frequency power source for CNTs growth
- APRFD creates stable continuous regime for CNTs growth, much lower operating voltage due to ion “trapping” between the electrodes, no dielectric barrier needed

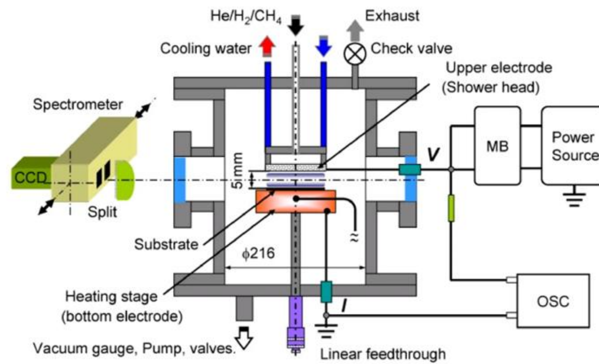

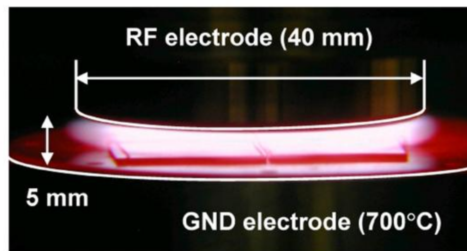

Figure 1. APRFD reactor and image of APRFD during CNT growth.

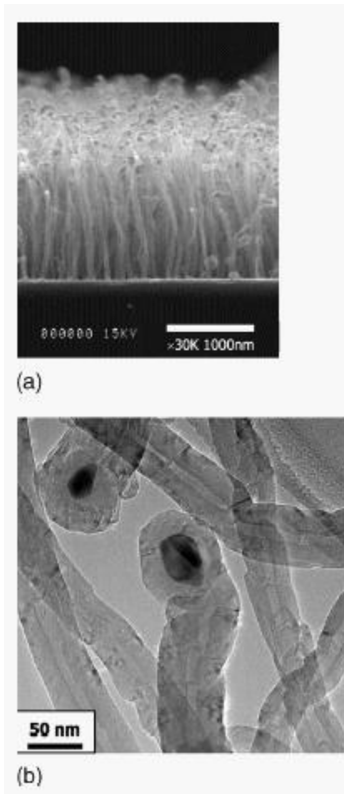

Parameters: 2 inch Si wafer <100> coated with Cr/Ni (20 nm/20 nm(sputtered)), Discharge area: 12.6 cm^2 Deposition time: 5, 10 , 20 min, $He/H_2/C_2H_2$ (1000/4-10/2 sccm)

CNTs growth in APGD

- Even with use of APRFD the growth of SWCNTs remained a challenge, key issue was the form of the catalyst
- In 2007 T. Nozaki, K. Ohnishi, K. Okazaki, U. Kortshagen. Carbon 45, 364 used densely mono-dispersed Fe–Co catalysts of a few nanometers size (first used by Maruyama) for aligned layers of SWCNTs
- Prepared nanoparticles were reduced in He/H_2 1500/10 sccm at APRFD at 400 °C for 5 min, then 15 min at 700°C, deposition $He/H_2/CH_4$ 1000/30/16 sccm for 5 min at 700 °C

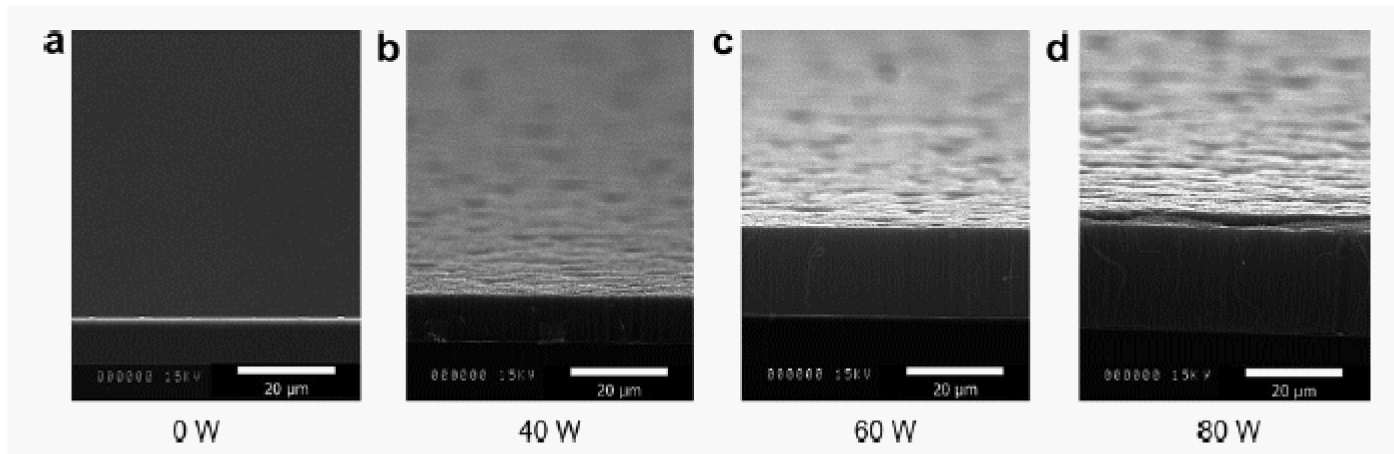

CNTs growth in APGD

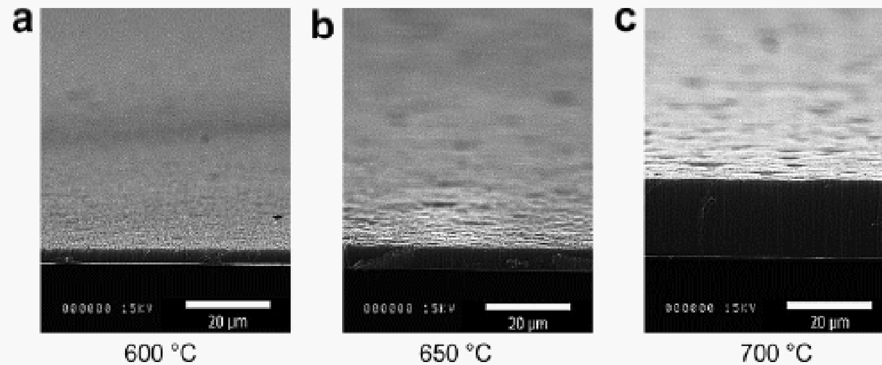

Fig. 8. SEM micrographs of SWCNTs at different substrate temperatures.

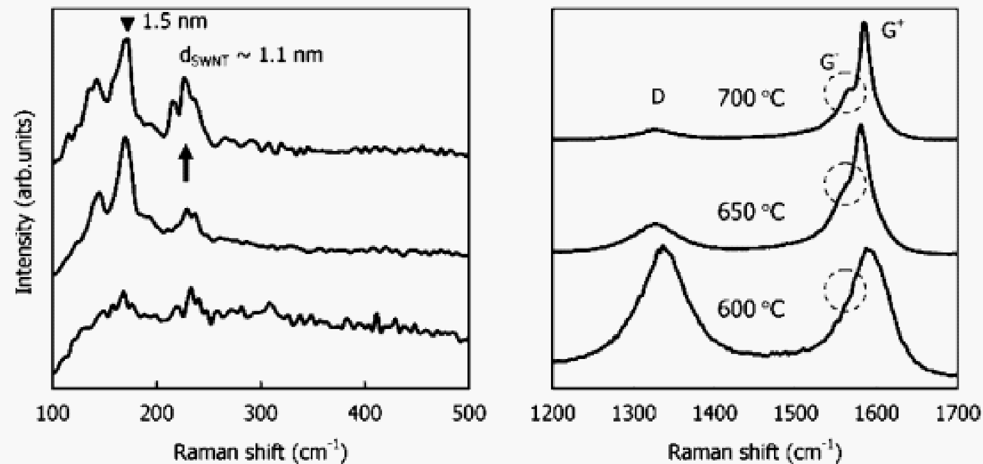

Fig. 9. Raman scattering spectra of samples shown in Fig. 8.

T. Nozaki, K. Okazaki, Carbon Nanotube Synthesis in Atmospheric Pressure Glow Discharge: A Review, Plasma Process. Polym. 2008, 5, 300–321

CNTs growth in APGD

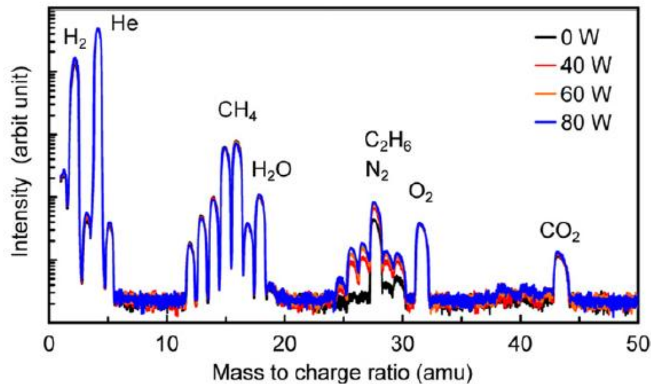

Figure 4. Mass spectrum of the reacting gas obtained directly from the sheath; conditions: $He/CH_4/H_2 = 1000/16/30\,cm^3\,min^{-1}$ and $700\,^{\circ}C$.

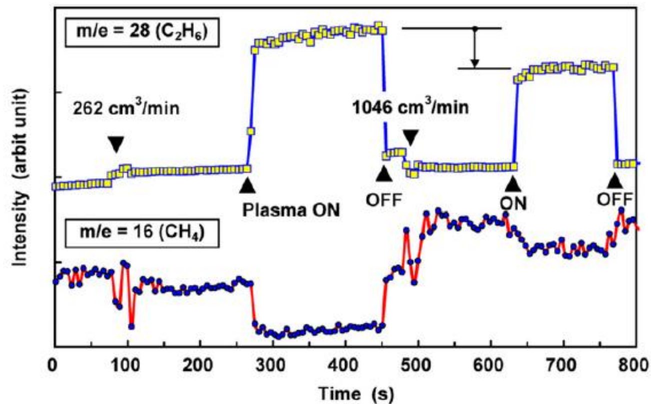

Figure 5. Time-dependent change-of-mass spectrum for $m/e = 16$ and 28. See figure 4 caption for the conditions.

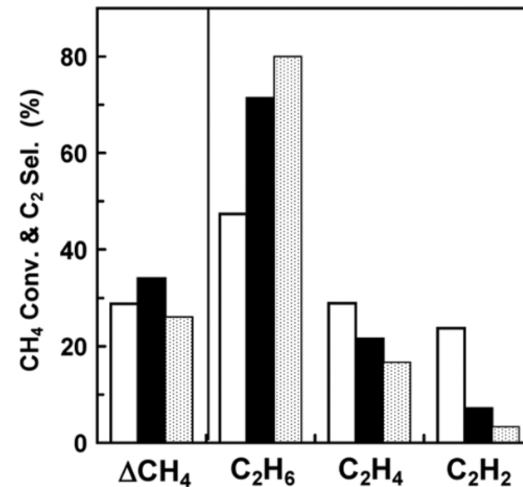

Figure 6. CH_4 conversion and selectivity for the C_2 hydrocarbon: □ 20 kPa, $H_2 = 0$; ■ 100 kPa, $H_2 = 0$; ░ 100 kPa, $H_2 = 90\,cm^3\,min^{-1}$; conditions: $He/CH_4 = 3000/48\,cm^3\,min^{-1}$ and 60 W.

T. Nozaki, S. Yoshida, T. Karatsu and K. Okazaki, Atmospheric-pressure plasma synthesis of carbon nanotubes, J. Phys. D: Appl. Phys. 44 (2011) 174007 (9pp).

CNTs growth in APG in $Ar/H_2/C_2H_2$

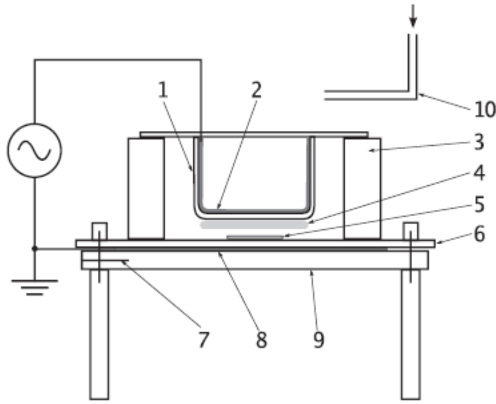

FIG. 1. Electrode configuration. 1—Simax glass dielectric, 2—upper electrode, 3—distance pillar, 4—discharge, 5—substrate, 6—AlN dielectric, 7—thermocouple, 8—bottom electrode, 9—heater, 10—gas inlet.

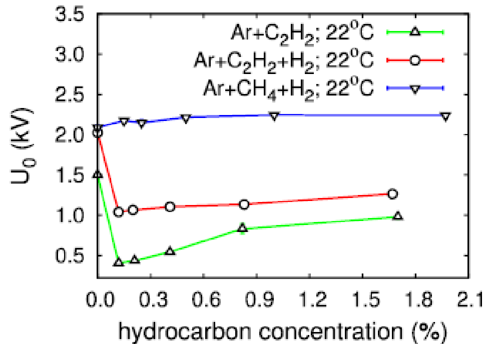

FIG. 2. The dependence of ignition voltage U_0 on the concentration or acetylene or methane added to Ar or Ar/H_2. The discharge was operated at room temperature 22 °C. Argon and hydrogen flow rates were 7 slm and 100 sccm, respectively.

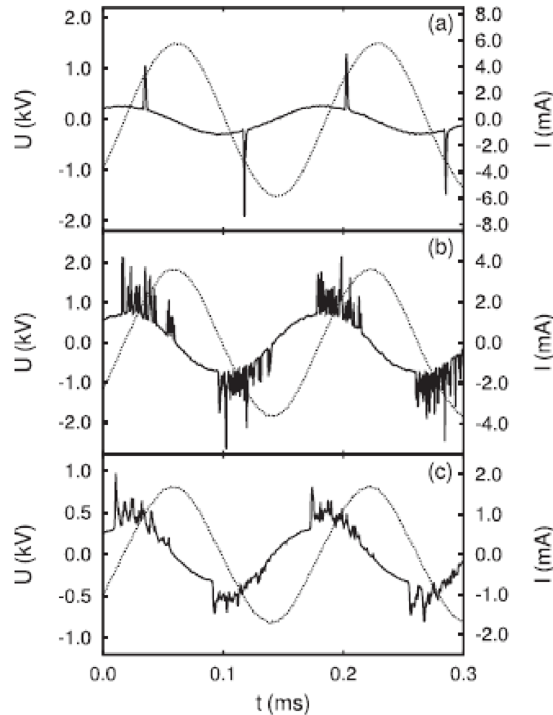

FIG. 3. The time dependence of applied voltage (dotted line) and discharge current (full line) at room temperature for (a) DBD in pure Ar, (b) DBD in Ar/CH_4, and (c) APGD in Ar/C_2H_2. The concentration of CH_4 or C_2H_2 in Ar was 0.41 vol. %. Discharges were operated slightly above the ignition voltage in particular gas mixture.

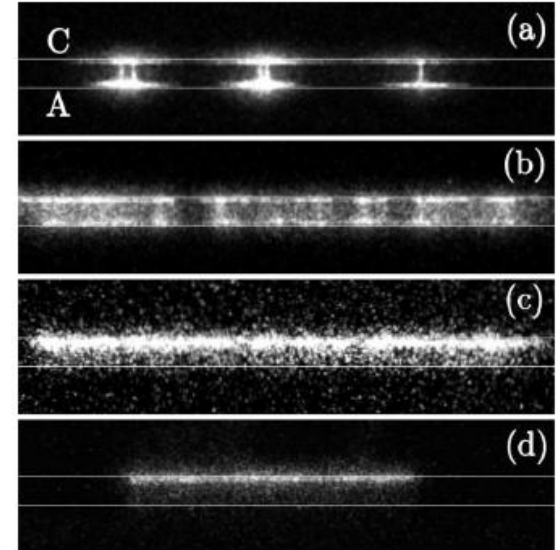

FIG. 5. ICCD images of discharges at room temperature with 80 μs (one half-period) exposure time: (a) filamentary DBD in Ar, (b) filamentary DBD in Ar/CH_4, (c) APGD in Ar/C_2H_2, and (d) APGD in $Ar/C_2H_2/H_2$. The concentration of CH_4 or C_2H_2 was 0.41 vol. %. Horizontal lines indicate the dielectric surfaces and the upper electrode is the instantaneous cathode in all images.

6,8 kHz power supply with 0.8–4.0 kV (peak-to-peak) voltage , electrode distance of 1,75 mm, 10x15 mm Si/SiO_2 (300 nm)/5 nm Fe catalytic layer. Ar/H2/CH_4 or C_2H_2 mixture.

Eliáš M., Kloc P., Jašek O., Mazánková V., Trunec D., Hrdý R., Zajíčková L., Atmospheric pressure barrier discharge at high temperature: Diagnostics and carbon nanotubes deposition, Journal of Applied Physics 117(10) (2015) 103301.

CNTs growth in APG in $Ar/H_2/C_2H_2$ – diagnostics at high temperature

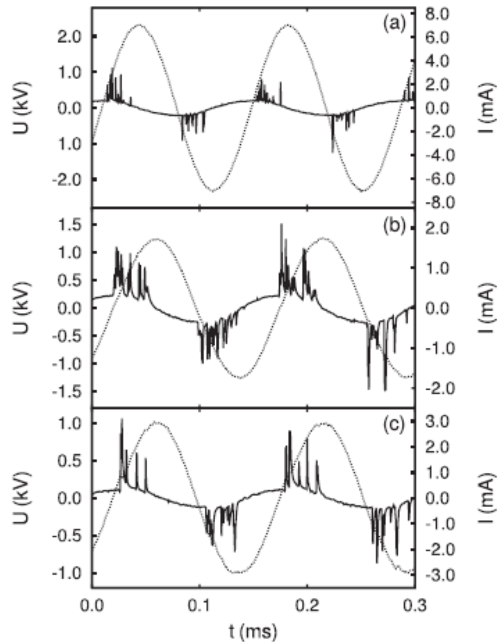

FIG. 4. The time dependence of applied voltage (dotted line) and discharge current (full line) for (a) DBD in $Ar/CH_4/H_2$ at 22 °C, (b) APGD $Ar/C_2H_2/H_2$ at 22 °C, and (c) APGD $Ar/C_2H_2/H_2$ at 680 °C. The concentration of CH_4 or C_2H_2 in Ar/H_2 was 0.41 vol. %. Discharges were operated slightly above the ignition voltage in particular gas mixture.

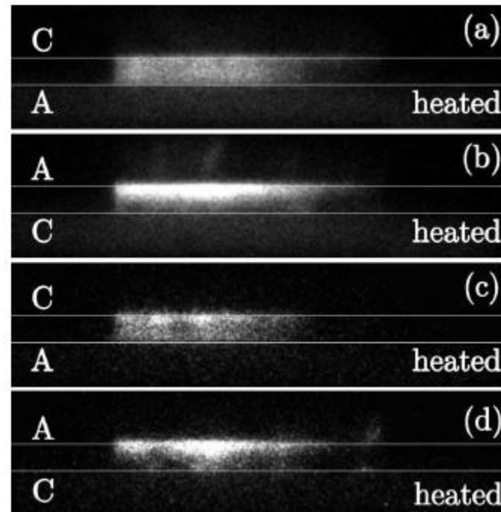

FIG. 8. ICCD images of APGD in $Ar/C_2H_2/H_2$ with 0.41 vol. % admixture of C_2H_2 and bottom electrode heated to 680 °C: (a) 80 μs (one half-period), instantaneous cathode at upper electrode, (b) 80 μs (one half-period), cathode at bottom electrode, (c) 5 μs, cathode at upper electrode, and (d) 5 μs, cathode at bottom electrode. Horizontal lines indicate the dielectric surfaces.

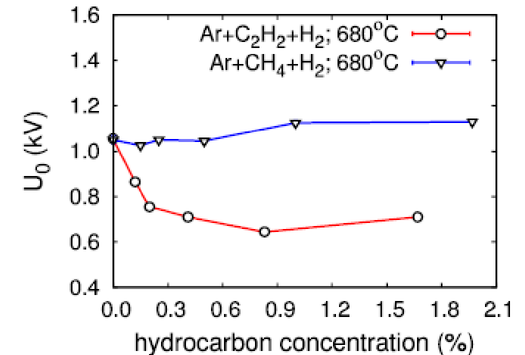

FIG. 7. The ignition voltage U_0 in dependence on the concentration of acetylene or methane added to Ar/H_2 for the temperature of bottom electrode 680 °C. Argon and hydrogen flow rates were 7 slm and 100 sccm, respectively.

If the bottom electrode was heated up to 680 °C the ignition voltage decreases due to the decrease of neutral gas concentration. Substrate temperature is 40 °C lower then heated electrode and upper electrode temperature is 250 °C lower. Due to the temperature profile the behaviour in instantaneous cathode or anode is different in each half period.

CNTs growth in APG in $Ar/H_2/C_2H_2$

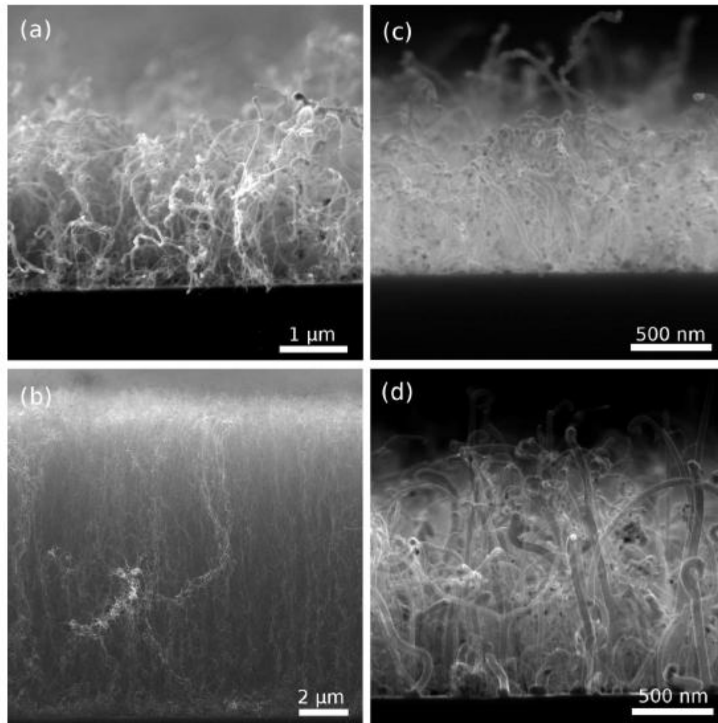

FIG. 13. Cross sectional SEM micrographs of deposited carbon nanostructures for (a) 0.1%, (b) 0.2% of C_2H_2 in $Ar/C_2H_2/H_2$ APG discharges, and (c) 0.2%, (d) 0.4% of CH_4 in $Ar/CH_4/H_2$ DBD discharges. The substrate temperature was 710 °C. The micrographs were made using TESCAN LYRA microscope.

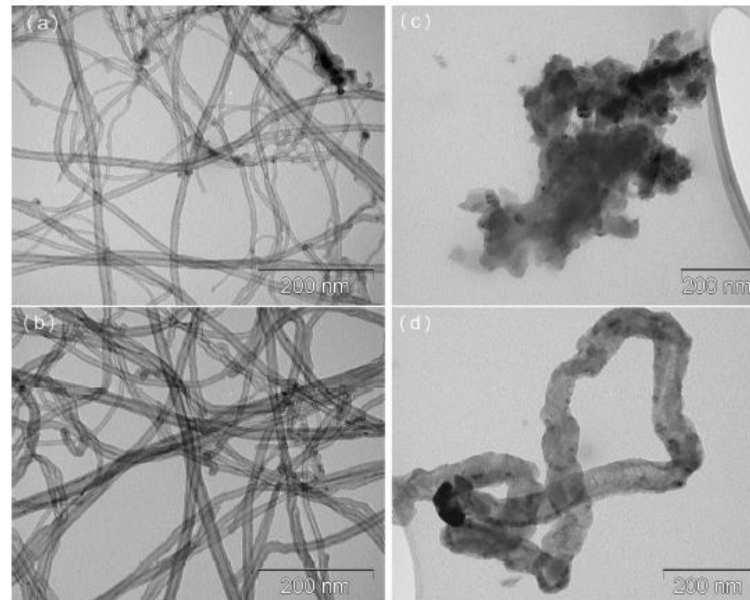

FIG. 12. TEM micrograph of the carbon nanostructures deposited from (a), (b) 0.2% of C_2H_2 in $Ar/C_2H_2/H_2$ mixture and (c), (d) 0.2% of CH_4 in $Ar/CH_4/H_2$ mixture. The substrate temperature was 610 °C for (a) and (c) and 710 °C for (b) and (d) images. The micrographs were made using Philips CM12 microscope.

CNTs deposition by plasma arcs/jets/torches at atmospheric pressure

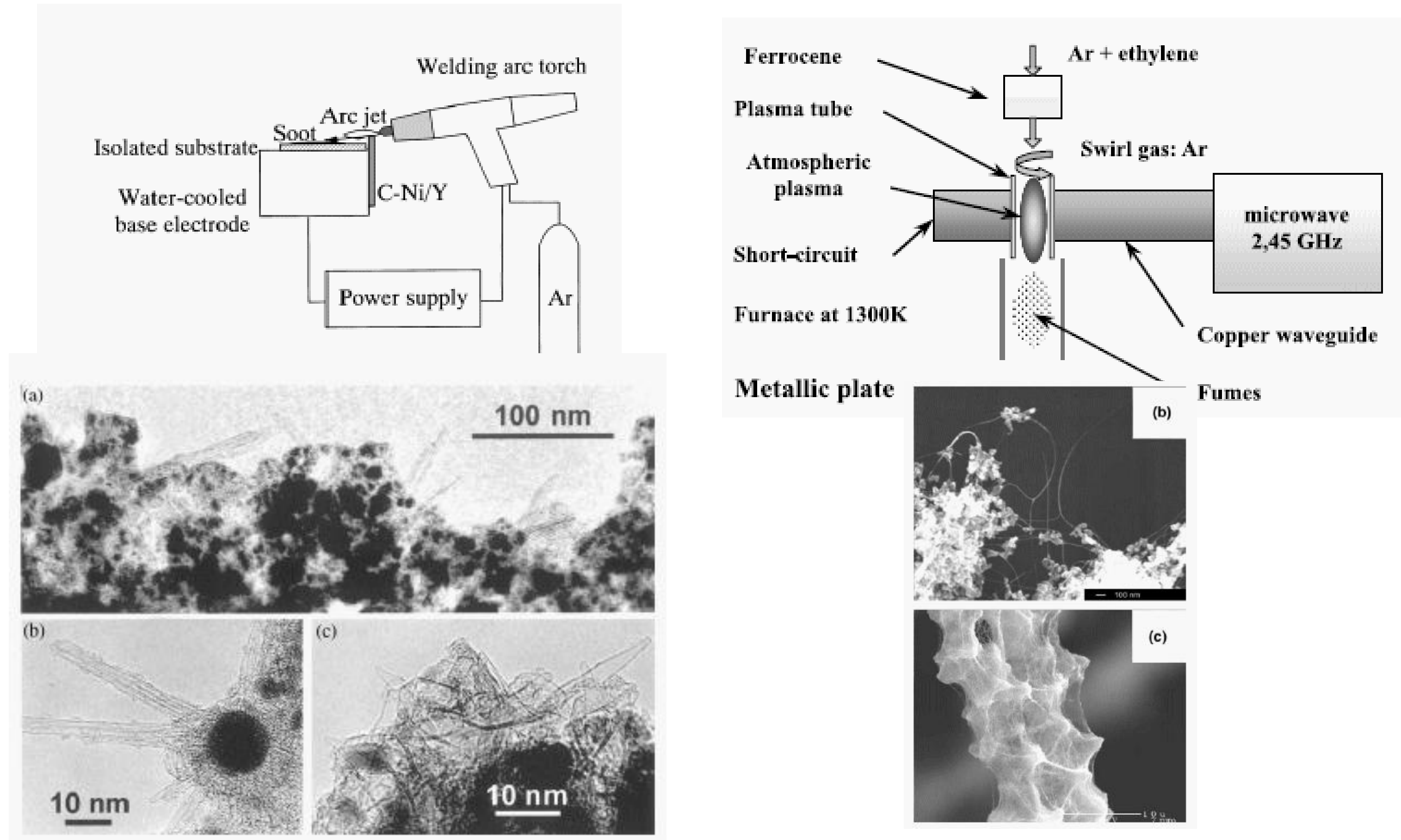

H. Takikawa et al. *Physica B* 323, 277 (2002)., O. Smiljanic et al., Chem. Phys. Lett. 356, 189 (2002).

CNTs deposition by plasma arcs/jets/torches at atmospheric pressure

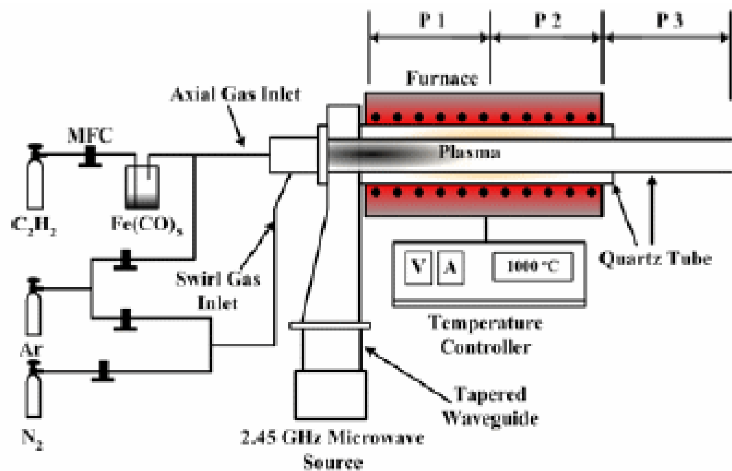

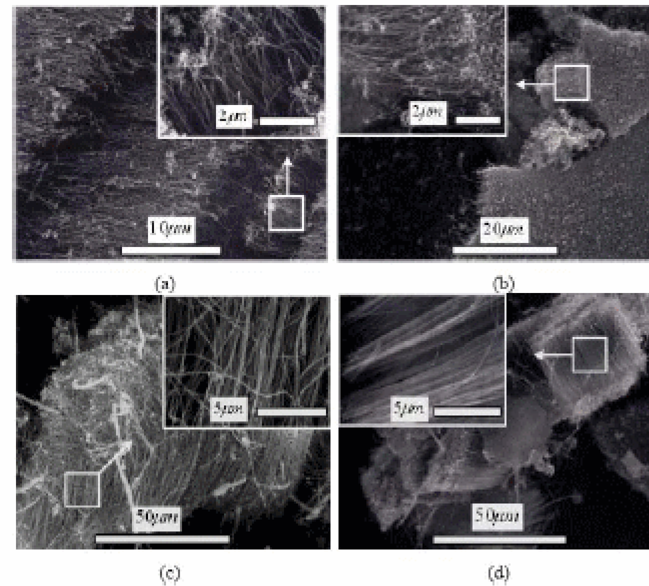

Fig. 9. SEM images of CNTs obtained from the atmospheric microwave plasma-torch. (a) at a furnace temperature of 700, (b) 800, (c) 900, and (d) 1000 °C.

Y. Ch. Hong, H. S. Uhm, Physics of plasmas 12, 053504 (2005)

CNTs synthesis by microwave plasma torch at atmospheric pressure

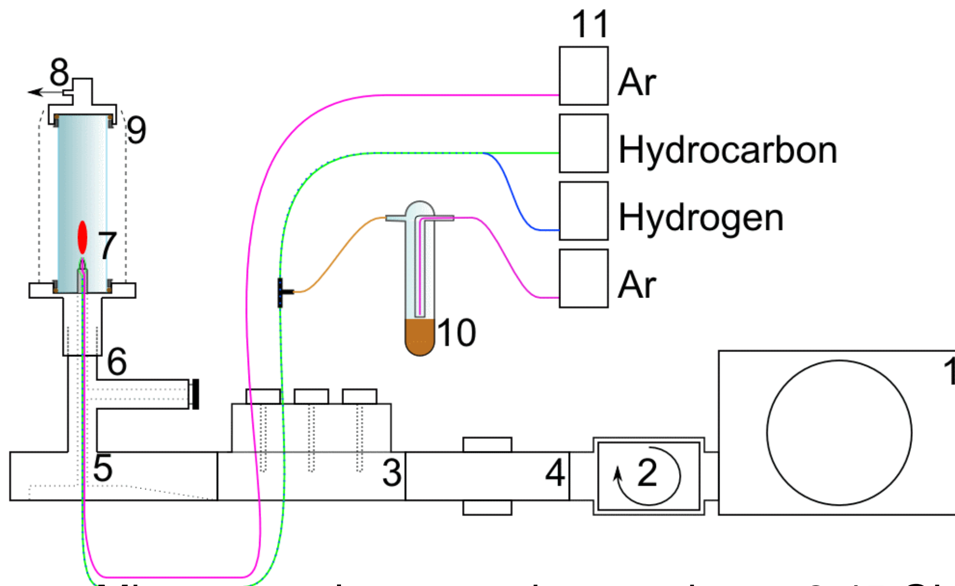

Microwave plasma torch operating at 2,45 GHz, max. 2 kW power, dual gas flow
Center - Ar(500-1500 sccm)/
Outer - H_2(250-500 sccm)/CH_4(10-50 sccm)
Si/Fe, Si/SiO_x/Fe, Si/Al_xO_y/Fe substrates
Fe(1-10 nm) vacuum evaporated, SiO_x PECVD
O. Jašek, M. Eliáš, L. Zajíčková et al., Materials Science and Eng. C, 26, 2006, 1189

CNTs synthesis by microwave plasma torch at atmospheric pressure

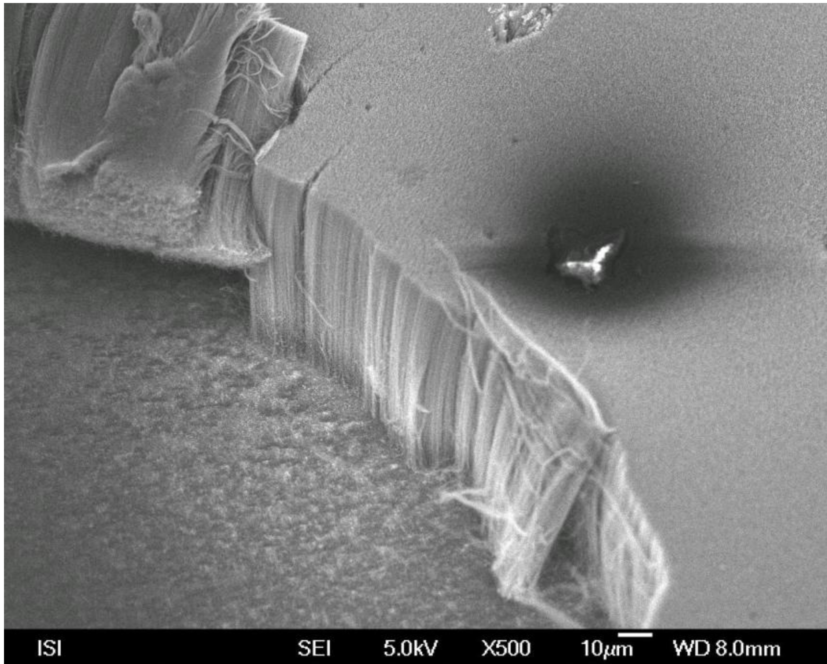

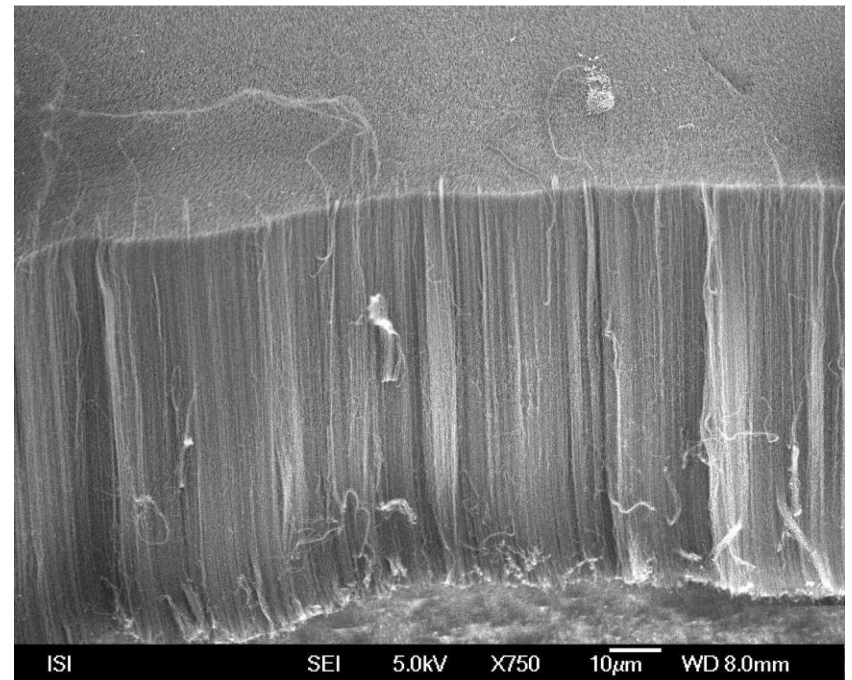

Substrate type Si/SiO_2/Fe 10 nm (Q_{CH4}=40 sccm, Q_{H2}=400 sccm, Ar=1500 sccm, T_S=700^0C, t_d=15 min.).

CNTs synthesis by microwave plasma torch at atmospheric pressure

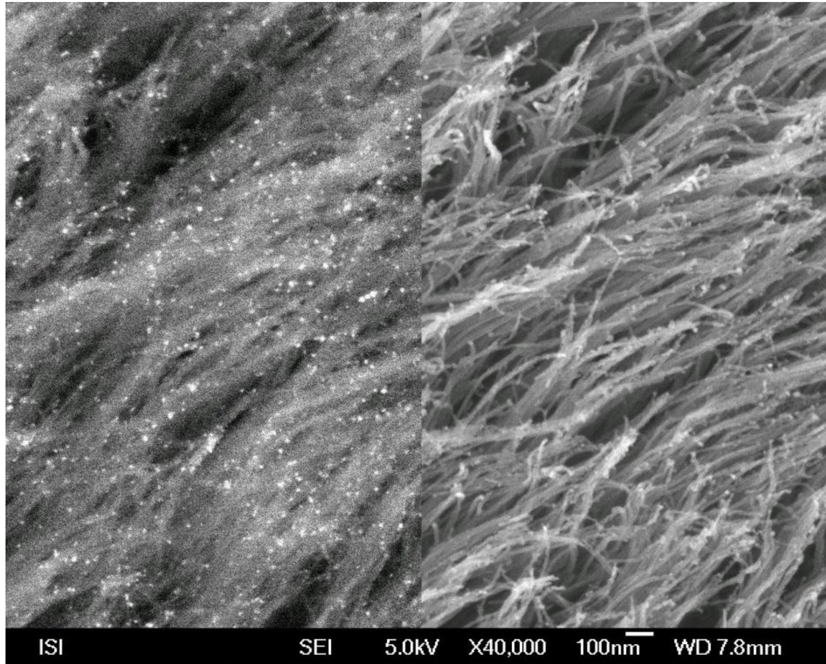

Material contrast analysis – comparison of micrographs in secondary and backscattered electrons. White points correspond to catalytic particles – tip growth mode.

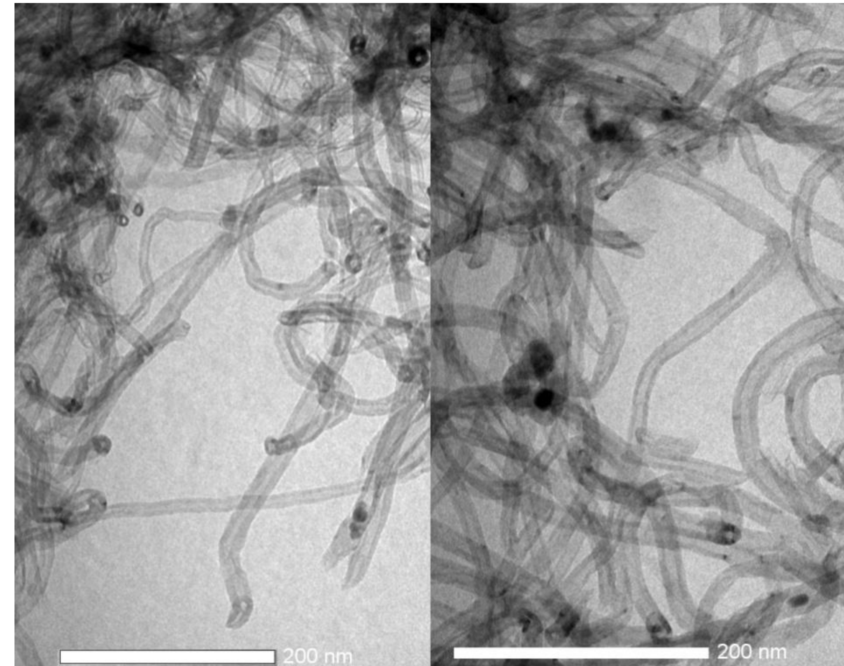

TEM micrograph

CNTs growth in microwave plasma torch with floating catalyst

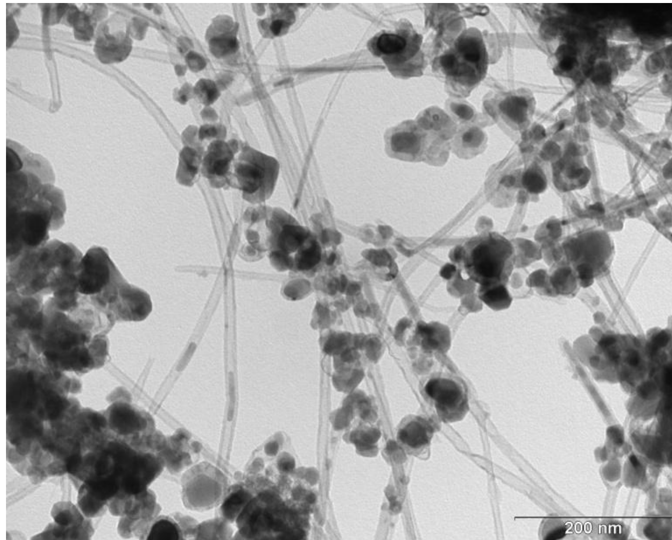

TEM micrograph of MWCNTs/SWCNTs deposited from mixture of $Ar/H_2/CH_4$ and $Fe(CO)_5$
Deposition of SWCNTs on the substrate using ethanol admixture

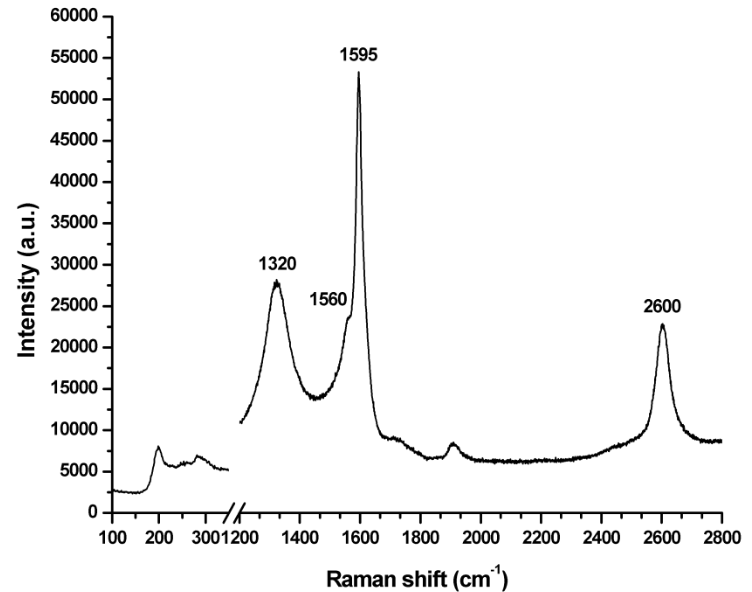

Raman spectra of deposited nanostructures

Methods of making graphene

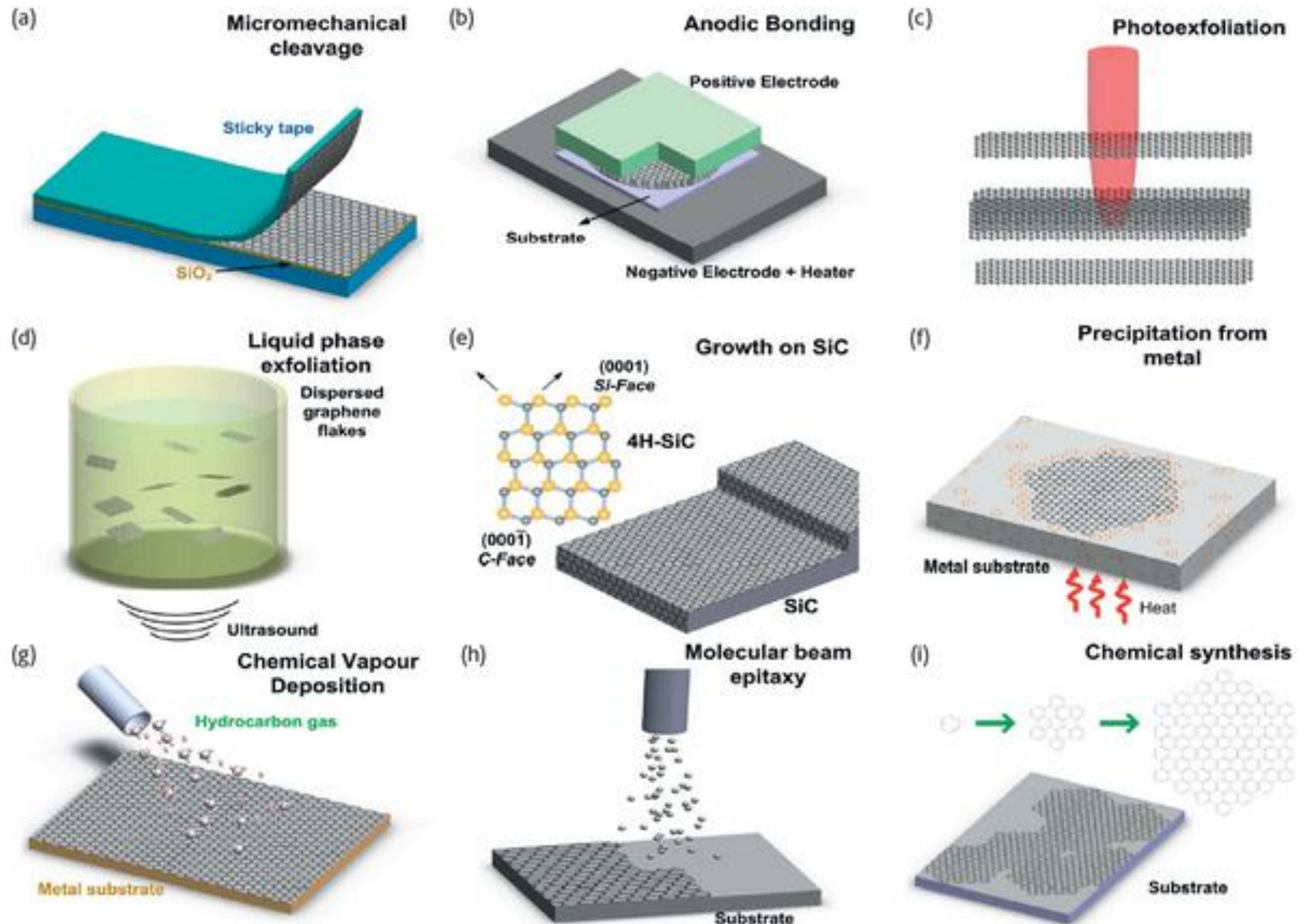

F. Bonaccorso et. al. Production and processing of graphene and 2d crystals, Materials Today 15(12), 2012, 564

Graphene deposition using plasma sources

- Synthesis of graphene on metalic or dielectric substrates by PECVD
- Synthesis of vertical aligned graphene nanosheets on substrates
- Synthesis in volume of the plasma discharge
- Plasma pretreatment – reduction of GO, cleaning of the substrate, functionalization of the deposition layer – graphane (H_2), graphene transfer

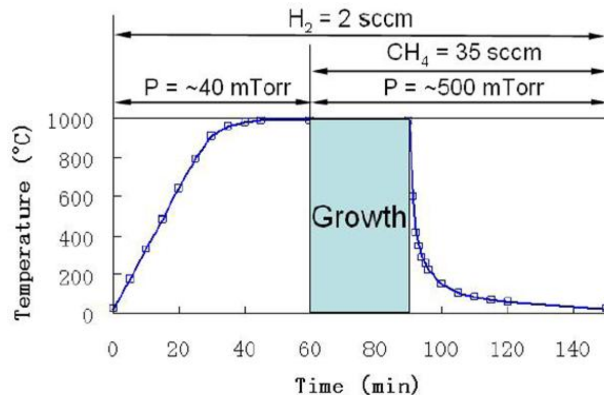

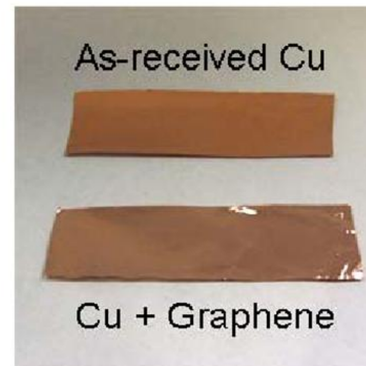

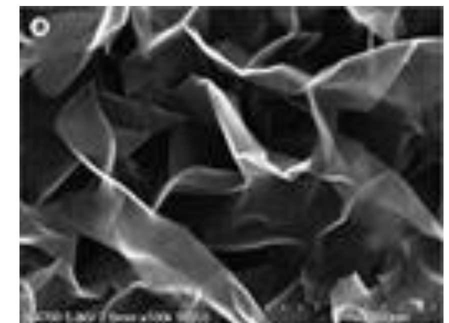

Graphene deposition using plasma sources

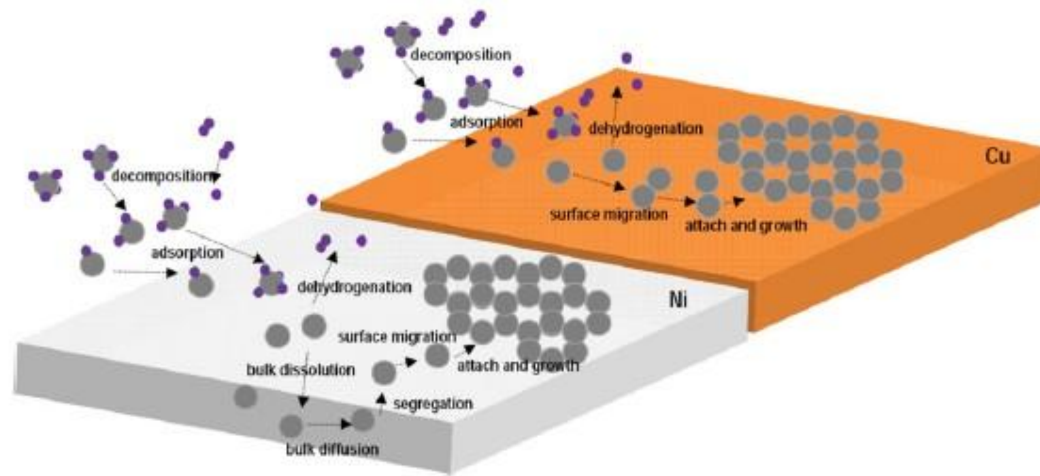

Fig. 2. Growth kinetics in CVD-produced graphene on various catalysts: Case of CH_4 on Ni and Cu.

R. Munoz and C. Gomez-Aleixandre, Review of CVD Synthesis of Graphene, Chem. Vap. Deposition 2013, 19, 297

Graphene deposition using plasma sources

Low pressure microwave plasma surface wave discharge.
Cu (30 μm),Al (12 μm), Ni foils pretreated in Ar/H_2 plasma at 5 Pa for 20 minutes. Deposition parameters: 3-4.5 kW MW power, deposition time 30-180 s in $CH_4/Ar/H_2$ 30/20/10 sccm mixture.

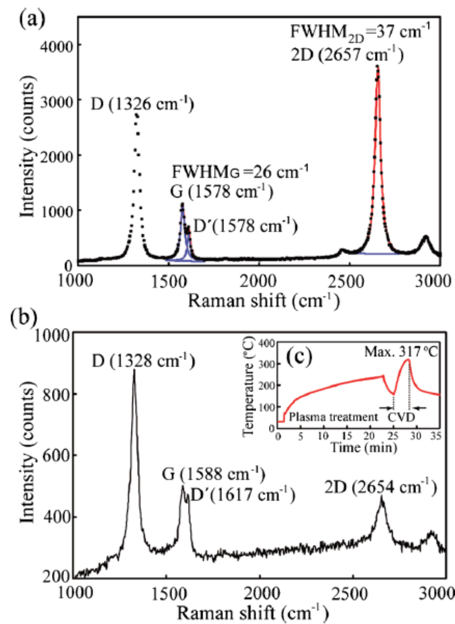

FIG. 1. (Color online) Raman spectra (638 nm laser, 1 μm spot size) o graphene-based films deposited at substrate temperatures below 400 °C b SWP-CVD. (a) Raman spectrum of a typical graphene-based film deposite on Cu foil (CVD conditions: 5 Pa, $CH_4/Ar/H_2$=30/20/10 SCCM, 3 kW per a MW generator, 30 s). (b) Raman spectrum of a graphene-base film deposited on Al foil (CVD conditions: 3 Pa, $CH_4/Ar/H$ =30/20/10 SCCM, 4 kW per a MW generator, 180 s). (c) Substrate tem perature profile during the Ar/H_2 plasma treatment and the plasma CVD fo the synthesis of the film on Al foil shown in Fig. 1(b).

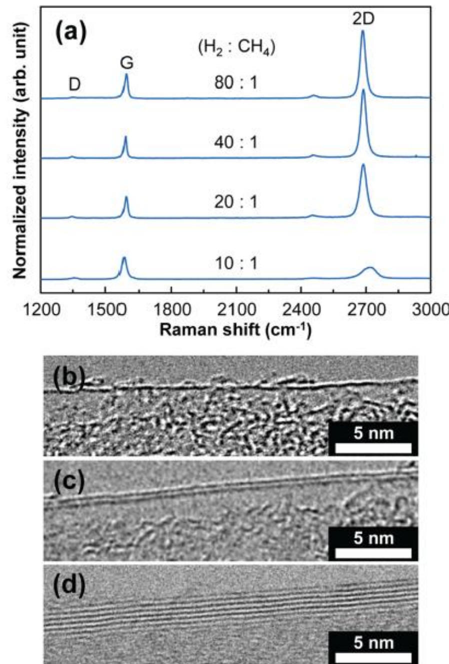

FIG. 1. (Color online) (a) Raman spectra taken at an excitation wavelength of 514 nm for the graphene films synthesized at various gas mixing ratio (synthesis time: 1 min, temperature: 750 °C). HR-TEM images of the graphene films synthesized at various gases mixing ratio: (b) 80:1 (H_2:CH_4), (c) 40:1, and (d) 10:1.

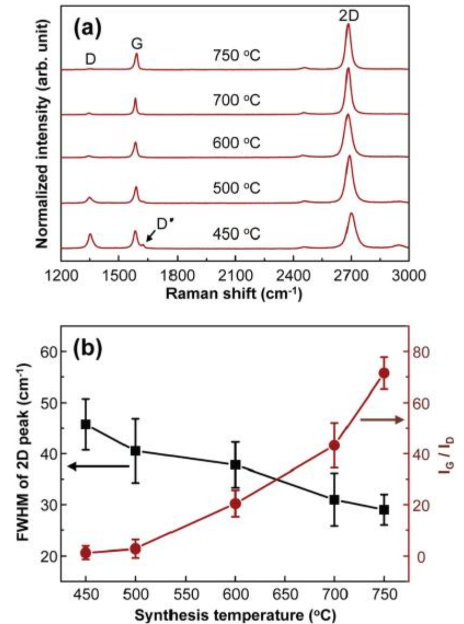

FIG. 2. (Color online) (a) Raman spectra taken at an excitation energy of 2.41 eV for the graphene synthesized at several synthesis temperatures (gas mixing ratio (H_2:CH_4): 80:1, synthesis time: 1 min). (b) FWHM of the 2D peak and the intensity ratio of the 2D peak compared to the G peak as a function of synthesis the temperature.

Y. Kim et al, Low-temperature synthesis of graphene on nickel foil by microwave plasma chemical vapor deposition, APPLIED PHYSICS LETTERS 98, 263106 (2011).
J. Kim et al., Low-temperature synthesis of large-area graphene-based transparent conductive films using surface wave plasma chemical vapor deposition, APPLIED PHYSICS LETTERS 98, 091502 2011.

Graphene deposition using plasma sources

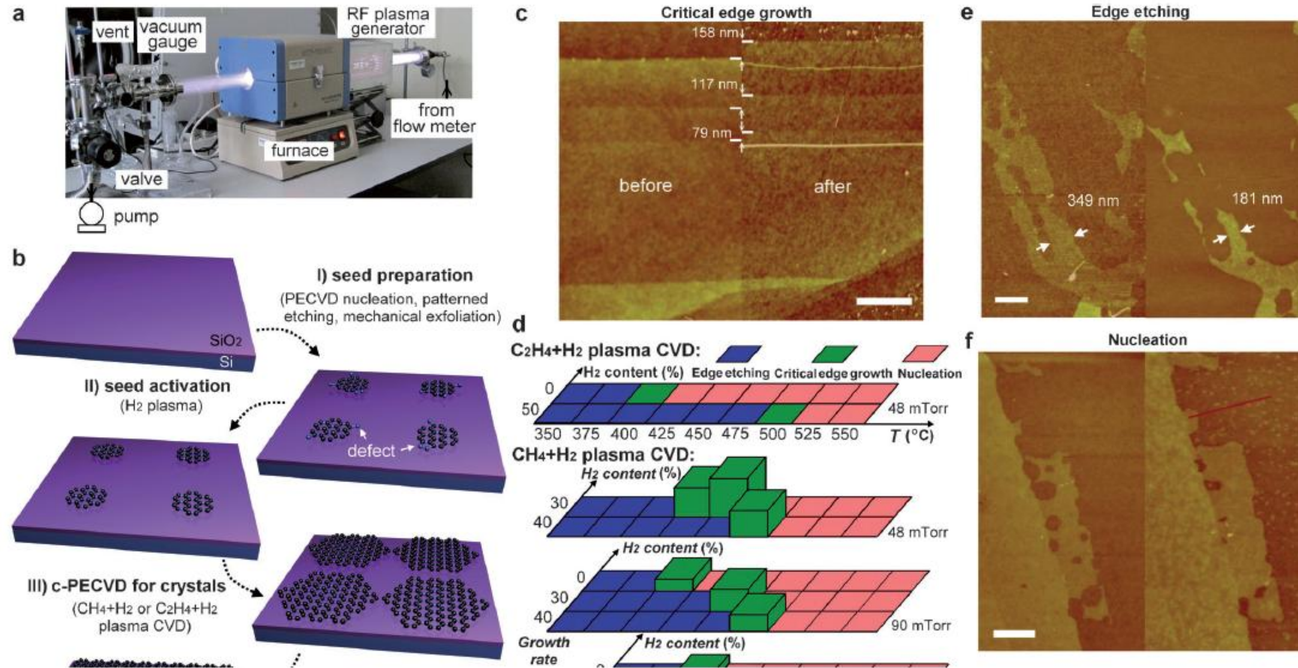

Figure 1. a) The remote radiofrequency (RF) PECVD system used. b) Schematic illustration of the c-PECVD procedure. c) AFM images of a peel-off graphene flake before (left) and after (right) c-PECVD. d) Plots of the experimental results as a function of the temperature (T) and H_2 content at 48, 90, and 300 mTorr. The blue, green, and red areas correspond to the parameters for edge etching, critical edge growth, and cluster nucleation, respectively. The height of the green columns indicates the growth rate. e,f) AFM images of peel-off graphene flakes after activation of the edges with a H_2 plasma (250 mTorr, 500°C) for 20 min (left columns), followed by CH_4+H_2 plasma CVD (30% H_2, 300 mTorr, 550°C) for 80 min (e, right column) or CH_4+H_2 plasma CVD (20% H_2, 300 mTorr, 600°C) for 40 min (f, right column). The height profile across the red line in the AFM image in (f) is shown below the AFM image. Scale bars (c,e,f): 500 nm.

RF PECVD remote plasma system with furnace and Si/SiO_2 substrate
D. Wei et al., Critical Crystal Growth of Graphene on Dielectric Substrates at Low Temperature for Electronic Devices, Angew. Chem. Int. Ed. 2013, 52, 14121 –14126.

Graphene deposition using plasma sources

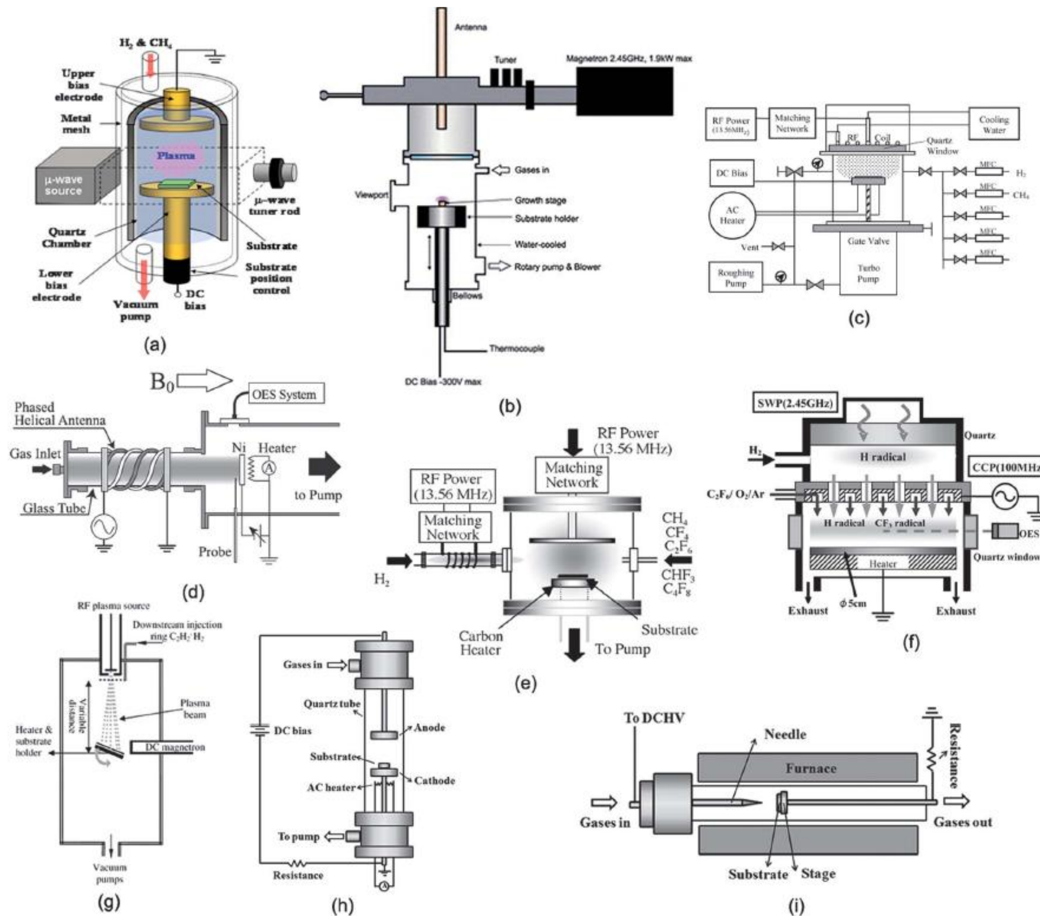

Fig. 1 Schematic diagrams of various PECVD systems for VG growth: (a) TE-MW (reprinted with permission from ref. 67; Copyright 2010 American Institute of Physics), (b) TM-MW (reprinted with permission from ref. 25; Copyright 2006 Elsevier), (c) ICP (reused with permission from ref. 68; Copyright (2004) Elsevier), (d) helicon plasma (reprinted with permission from ref. 24; Copyright 2006 Japan Society of Applied Physics), (e) CCP + ICP (reused with permission from ref. 69; Copyright 2005 Elsevier), (f) VHFCCP + MW (reprinted with permission from ref. 29; Copyright 2008 American Institute of Physics), (g) expanding CCP (reprinted with permission from ref. 70; Copyright 2010 Institute of Physics Publishing), (h) parallel-plate dc glow discharge plasma, and (i) pin-to-plate normal glow discharge plasma.

Z. Bo et al., Plasma-enhanced chemical vapor deposition synthesis of vertically oriented graphene nanosheets, Nanoscale, 2013, 5, 5180.

Graphene deposition using plasma sources

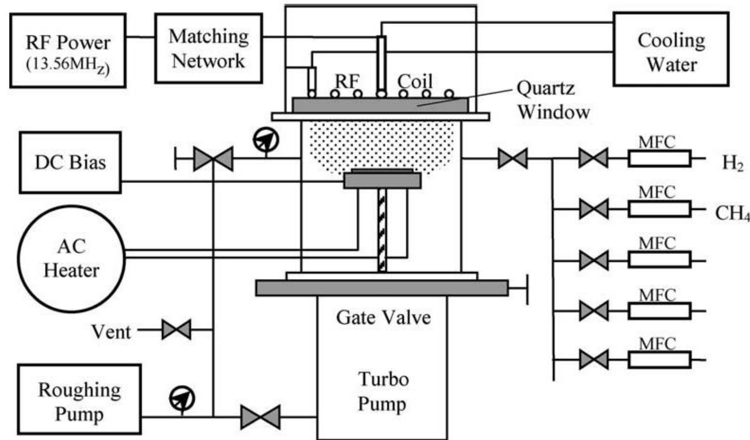

Fig. 1. Schematic of the inductively coupled RF PECVD system used for carbon nanosheet depositioi

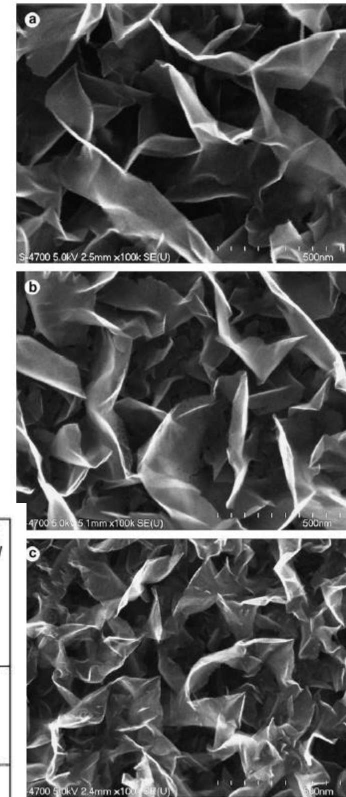

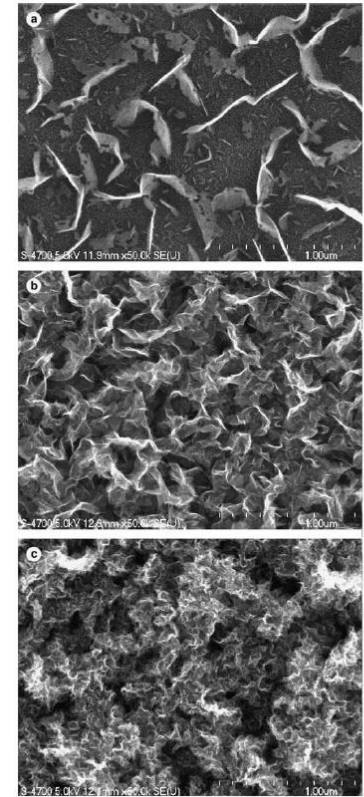

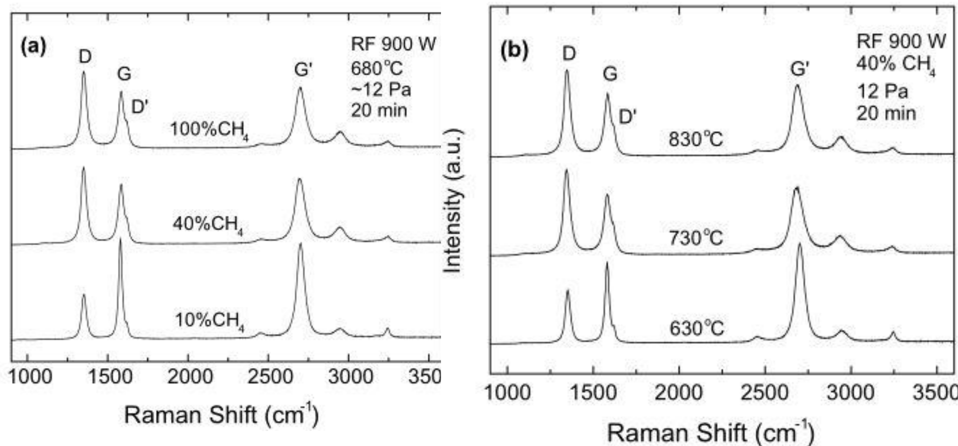

EM images of carbon nanosheets grown at different CH_4 tions on Si substrates: (a) 10% CH_4; (b) 40% CH_4; (c) 100% er deposition conditions are RF 900 W, 680 °C, ~12 Pa,

Fig. 3. SEM images of carbon nanosheets grown at different substrate temperatures on Si substrates: (a) 630 °C; (b) 730 °C; (c) 830 °C. Other deposition conditions are RF 900 W, 40% CH_4, 12 Pa, 20 min.

J. Wang et.al. Synthesis of carbon nanosheets by inductively coupled radio-frequency plasma enhanced chemical vapor deposition, Carbon 42 (2004) 2867–2872.

RF ICP CVD 13,56 MHz 900 W, 12 Pa, H_2/CH_4 mixture . Substrate Si, SiO_2, Al_2O_3, Mo, Cu etc.

Graphene deposition using plasma sources

Plasma source	Precursor	Growth pressure/Pa	Substrate temperature/°C	Flow rate/sccm[a]	Gas ratio
Helicon	CH_4	0.04–2	700	—	—
ICP	CH_4	12	630–830	10	—
ICP	CH_4/Ar	0.3	400	30.4	16.4 : 14
TM-MW	CH_4/Ar	17.33	450–500	—	1 : 8
TM-MW	CH_4/N_2	5.32×10^3	1250	—	—
TM-MW	CH_4/N_2	5.32×10^3	>1000	—	—
TM-MW	$C_2H_2/N_2/Ar$	1.33×10^4	650–1050	200	0.5% C_2H_2
TM-MW	$CH_4/N_2/Ar$	1.33×10^4	650–1050	200	4% CH_4
ICP	CH_4/H_2	12	630–830	10	>1 : 9
ICP	CH_4/H_2	2.66–53.2	600–950	—	>1 : 19
ICP	CH_4/H_2	13.33	700	10	2 : 3
ICP	C_2H_2/H_2	4–5.33	550–600	5	4 : 1
TE-MW	CH_4/H_2	133	650–700	50	1 : 4
TE-MW	CH_4/H_2	220	550	—	1 : 20
TE-MW	CO/H_2	250	700	50	23 : 2
TM-MW	CH_4/H_2	5.32×10^3	700	200	1 : 8
TM-MW	$CH_4/H_2/Ar$	1.33×10^4	650	44	1 : 1 : 20
TM-MW	C_2H_2/NH_3	1.33×10^3	—	—	>1 : 1
TE-MW[b]	CH_4/CO_2	—	900	—	53 : 47
Expending CCP[b]	$C_2H_2/H_2/Ar$	—	700	1076	1 : 25 : 1050
CCP + ICP	CH_4/H_2	13.3	500	45	1 : 2
CCP + ICP	CF_4/H_2	13.3	500	45	1 : 2
CCP + ICP	CHF_3/H_2	13.3	500	45	1 : 2
CCP + ICP	C_2F_6/H_2	13.3	500	45	1 : 2
VHFCCP + MW	C_2F_6/H_2	13.3–1596	600	150	1 : 2
VHFCCP + MW	$C_2F_6/H_2/N_2$	13.3–1596	600	155	10 : 20 : 1
VHFCCP + MW	$C_2F_6/H_2/O_2$	13.3–1596	600	155	10 : 20 : 1
DC glow	CH_4/H_2	1×10^4	1000	—	1 : 9
DC glow	CH_4/H_2	9975	1000	—	8 : 92
DC glow[c]	CH_4/H_2	2.66×10^4	900–1000	50	3–8% CH_4
DC glow[b]	$CH_4/H_2/Ar$	1.3	550–800	87	1 : 1.25 : 5
DC glow	$CH_4/H_2O/Ar$	1.01×10^5	700	1500	10% CH_4[d]

Best quality sheets according to Raman spectroscopy produced by MW-PECVD with FWHM of 2D peak of 25-55 cm^{-1} and I_D/I_G ratio of 0.2-0.3.

Graphene deposition using plasma sources

Growth rate:
Highest growth rates are achieved with MW sources, up to 96 μm.h^{-1}, then ICP 16 μm.h^{-1} and lowest with CCP and DC glow 0.1-1 μm.h^{-1}. With increasing power more CH_x, C_2 and H or CF_x species are created. C_2 with concentration of 10^{11}-10^{13} cm^{-3} is being considered as critical for nucleation of sheets.

Etchant in the deposition mixture: NH_3, H_2, O_2, CO_2 or H_2O
Quality of the sheets can be influence by removal of defects during the growth. This is usually accomplished by introducing NH_3 or O related compound.
Such admixture needs to be carefully dosed and optimized, otherwise all the deposit will be etched away.

Patterned growth:
Patterned catalyst layers of Ti, Co, Pt, Fe or Au or biasing of such patterns.
Vertical growth is not oriented in the beginning but with growing density the structure becomes oriented with help of **electric field**.

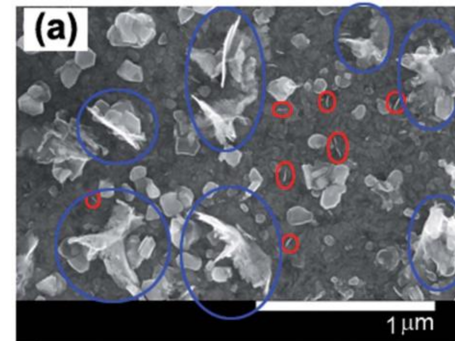

18.9 % H_2O

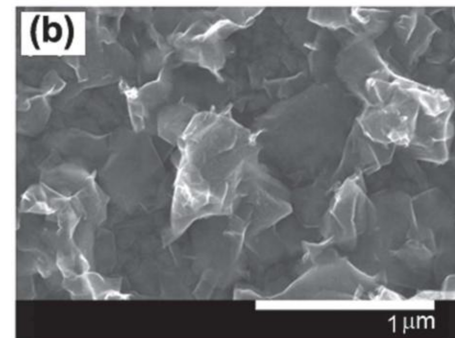

38.8 % H_2O

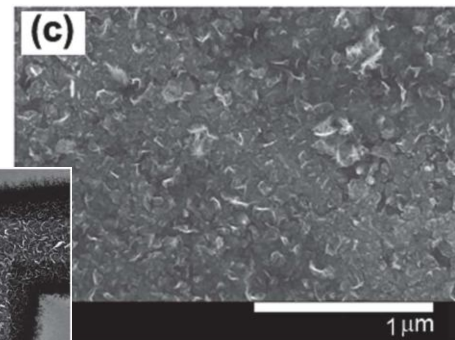

62.1 % H_2O

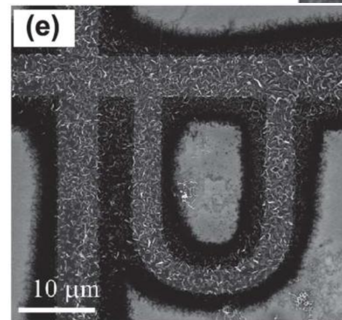

Graphene synthesis in microwave plasma at atmospheric pressure

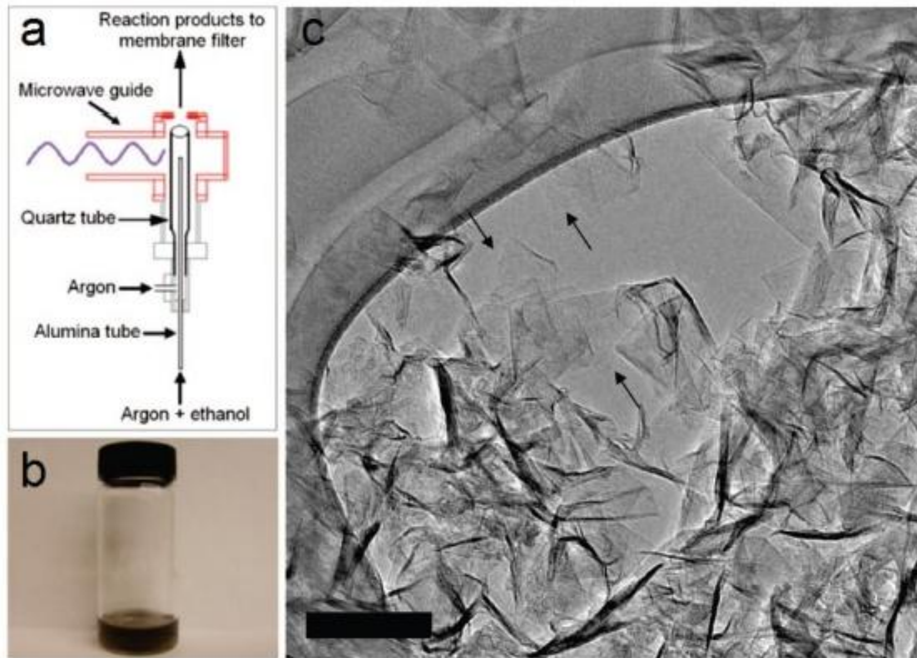

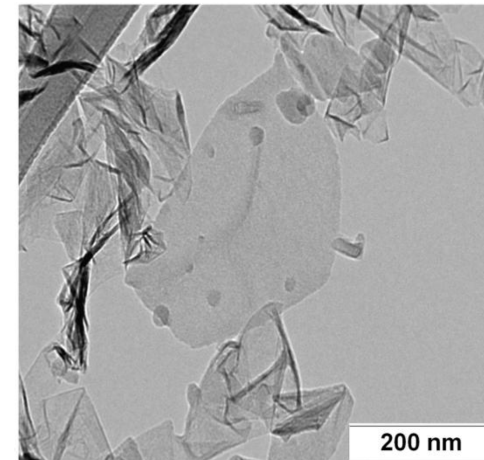

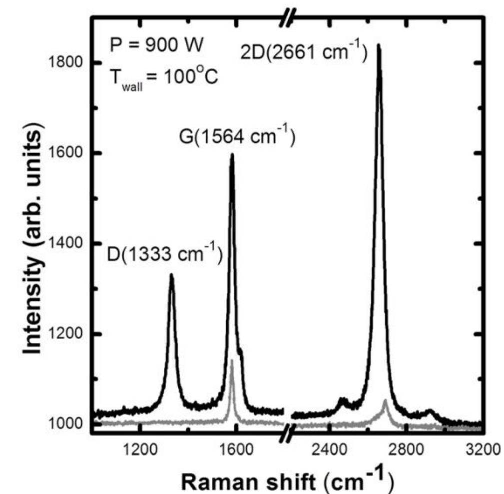

Decomposition of ethanol C_2H_5OH or dimethylether CH_3OCH_3 leads to formation of graphene sheets.
For the formation of nanosheets C_2 molecule is key reactive species, on the other hand free C atoms lead to formation of amorphous phase.

A. Dato, V. Radmilovic, Z. Lee, J. Phillips, and M. Frenklach, Substrate-Free Gas-Phase Synthesis of Graphene Sheets, Nano Letters, 8 (7), 2008, 2012.
A. Dato, M. Frenklach, Substrate-free microwave synthesis of graphene: experimental conditions and hydrocarbon precursors. New Journal of Physics, 2010, 12.12: 125013.
E. Tatarova et al. Microwave plasma based single step method for free standing graphene synthesis at atmospheric conditions. *Applied Physics Letters*, 2013, 103.13: 134101.

Graphene synthesis in volume at atmospheric pressure

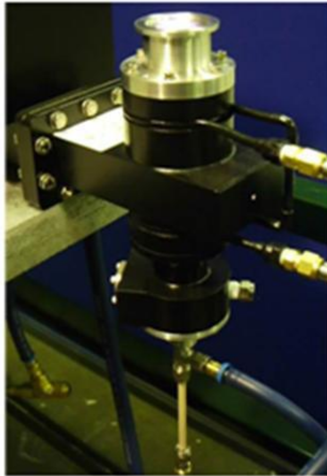

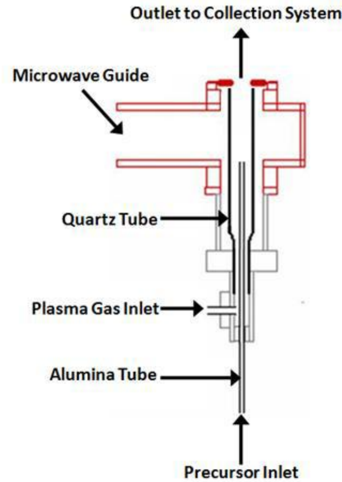

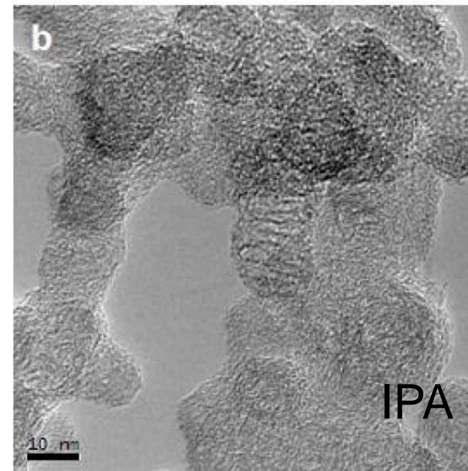

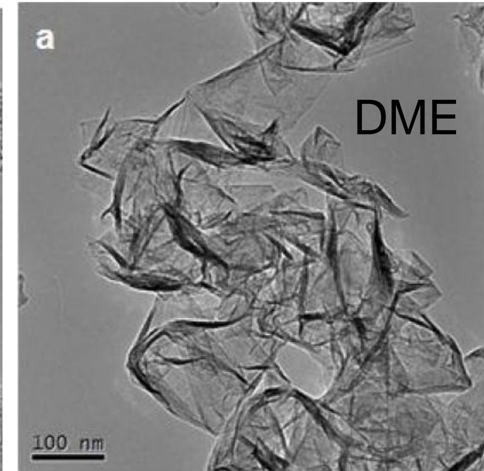

Liquid ethanol CH3-CH2OH
dimethylether (DME) CH_3OCH_3
methanol CH3-OH
isopropyl alcohol (IPA) $(CH_3)_2CHOH$
Ar flow ~ slm, precursor flow 0.1-1 sccm,
~ mg.min^{-1} and increasing with mw power, with lower flowrates - increasing residential time leads to increase of amorphous carbon content

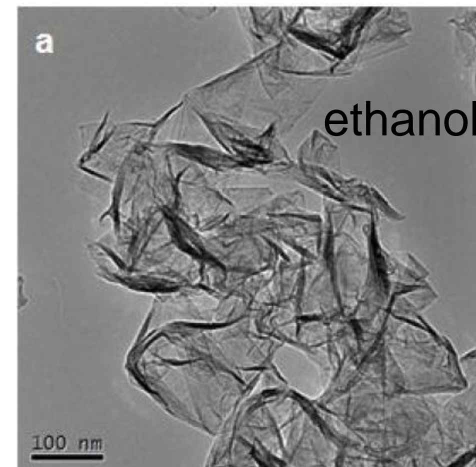

Graphene synthesis in volume at atmospheric pressure growth mechanism

•**Soot (amorphous carbon)** particles are formed from polycyclic aromatic hydrocarbon (PAH).

•**There is fine balance between C, O,H in different precursor.**
•Higher alcohols traditional create more soot, in case simplest alcohol, methanol, the generation of CHx hinders generation of C-C species, also in case the C/O ratio is close to 1, CO is usually formed. So with higher alcohols there is more C atoms and C-C bond can be formed.
•So for the IPA, because of abundance of C atoms PAH are formed while for ethanol and DME, the ratio is just right to generate appropriate amount of C-C species for graphene growth.

•**C/H ratio** also plays role in the growth but its influence is more complicated, but amount of H is related to generation of free C atoms and C_2 molecules.
•Some defects can be stabilized by H atoms but most edge defects are stabilized by curving and closure of a graphite sheet or generation of topological defects – pentagons.

•**High energy electrons** play role in case, if high mw power is used, and could be responsible for more PAH formation.

Microwave plasma torch

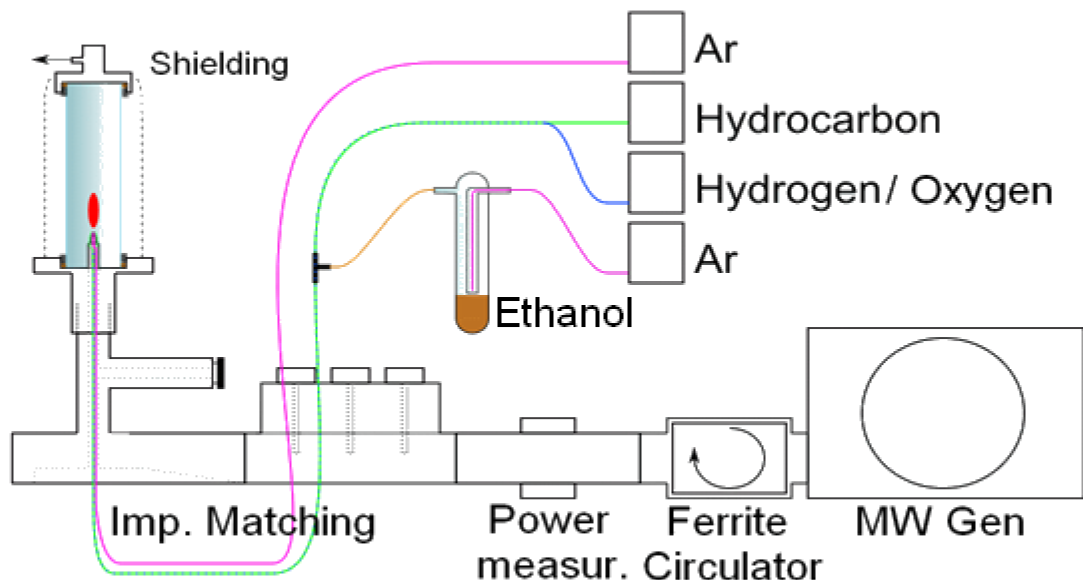

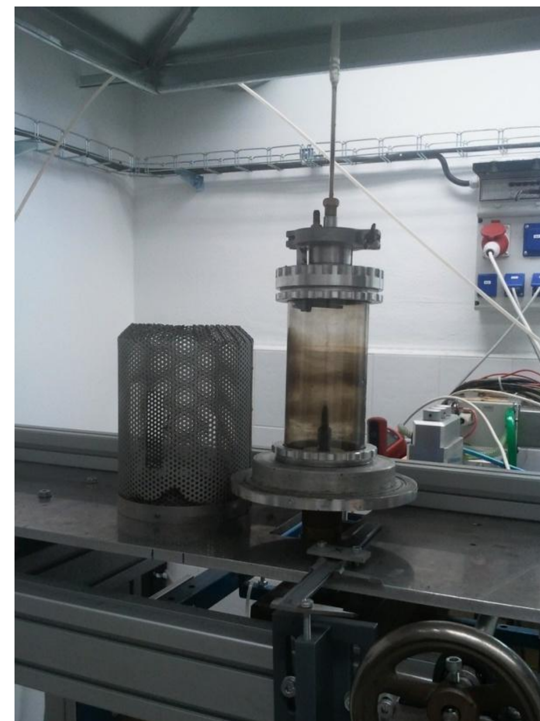

Microwave plasma torch operating at 2,45 GHz, (100 – 300 W) max. 2 kW power
Stainless dual channel nozzle (1 mm diameter)
Gas flows: center channel - Ar(100-1000 sccm)/ Outer channel Ar/ethanol (Ar 100-2800 sccm , 0.020 – 0.035 g/min of ethanol), admixture of O_2, H_2.
Deposition chamber consists of quartz tube 8 cm in diameter and 20 cm length with aluminum flanges. Upper flange includes gas exhaust and substrate holder.
Deposition can be carried out in volume or on substrates.

Microwave plasma torch

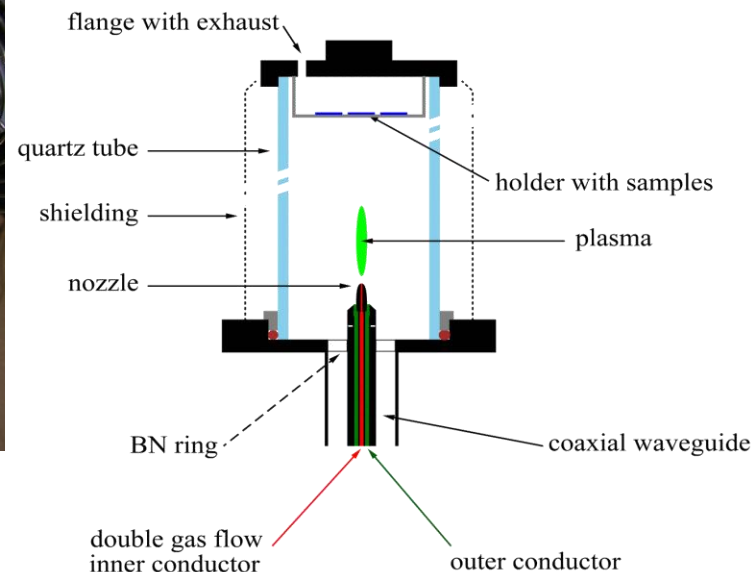

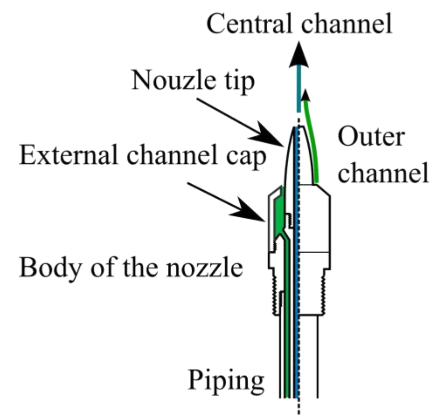

Neutral gas temperature up to 1800 K for Ar, and up to 4500 K in Ar/H_2

$n_e \sim 10^{20} - 10^{21}\ m^{-3}$

Graphene nanosheets synthesis in gas phase at atmospheric pressure

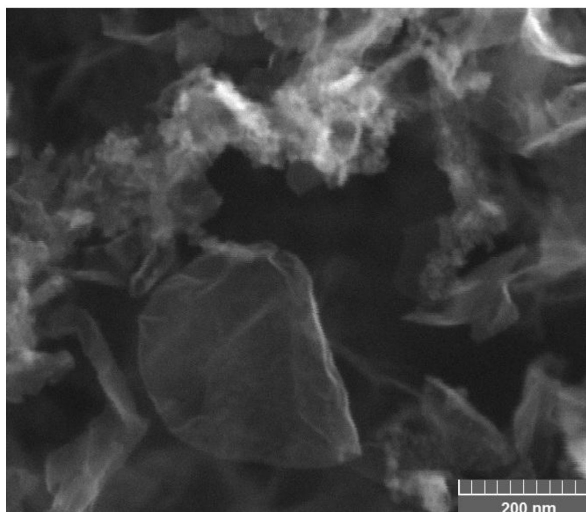

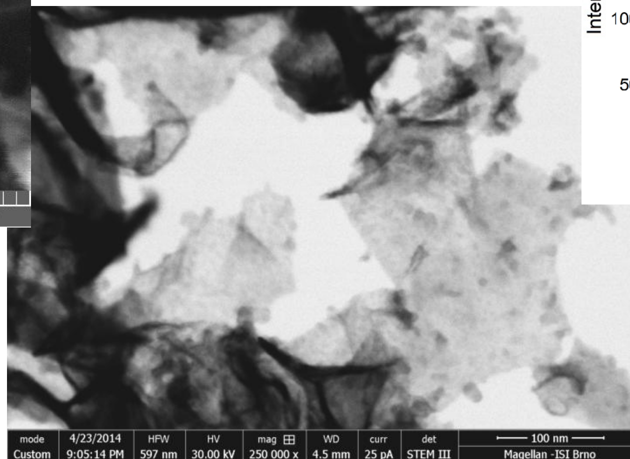

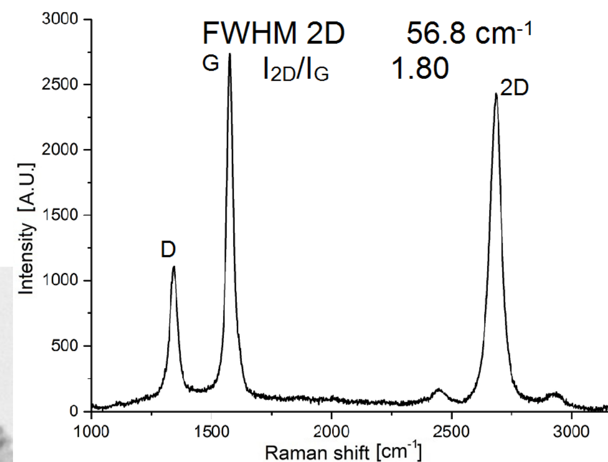

Ar_c 500 sccm, Ar_b 700 sccm, 210 W, 10 minutes

Graphene nanosheets synthesis in gas phase at atmospheric pressure

Ar_b/Ar_c flow rates

Ethanol delivery throught central channel results in deposition of smaller nanosheets in higher amount with amorphous carbon fraction. The discharge is also unstable and deposit is contaminated with iron nanoparticles from nozzle.

Argon flow rates and their ratio influence in our current setup mixing of precursor into plasma zone where nanosheet growth occurs.

At lower flowrates multi layer graphite sheets are synthesized and with increasing Ar_b/Ar_c ratio the higher quality graphene nanosheets are generared.

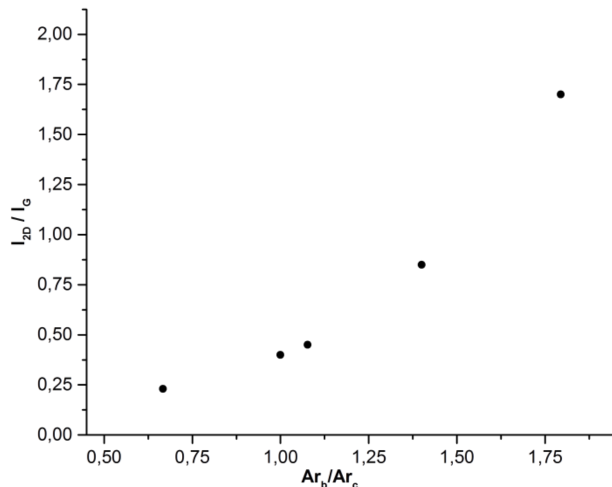

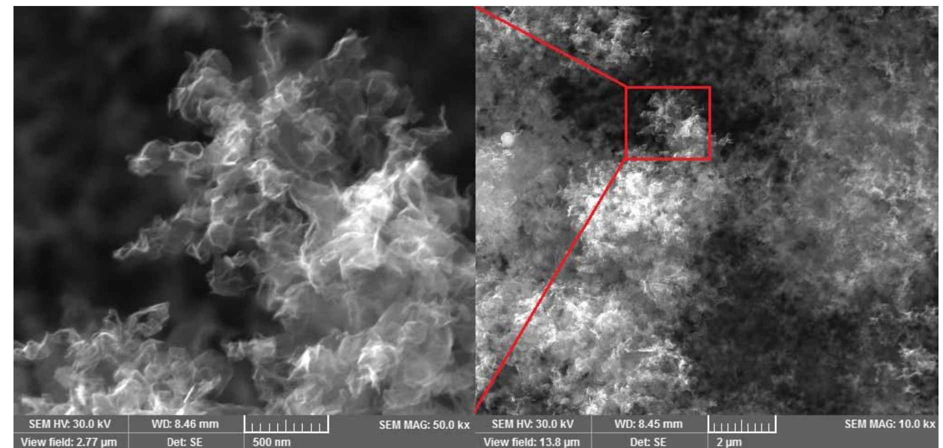

Higher ethanol flow rate into central channel

Graphene nanosheets synthesis in gas phase at atmospheric pressure

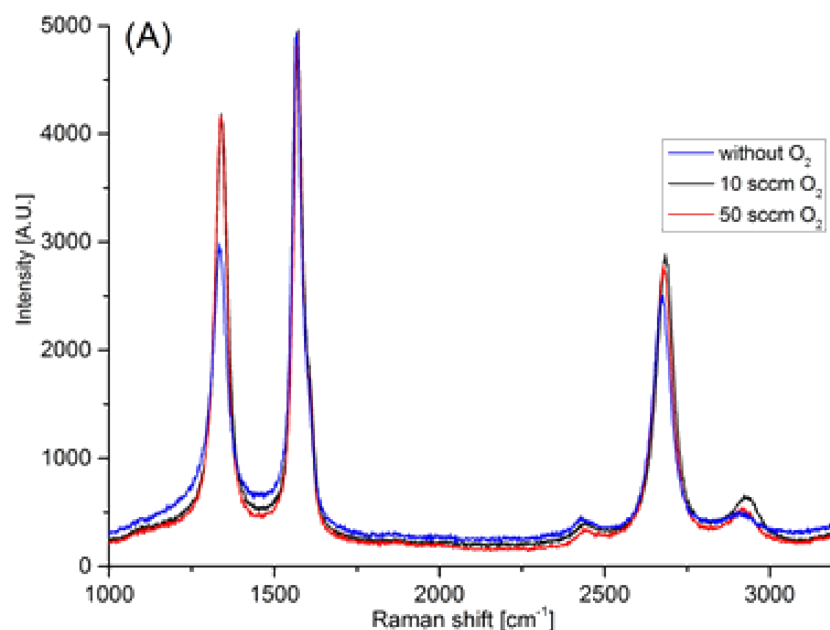

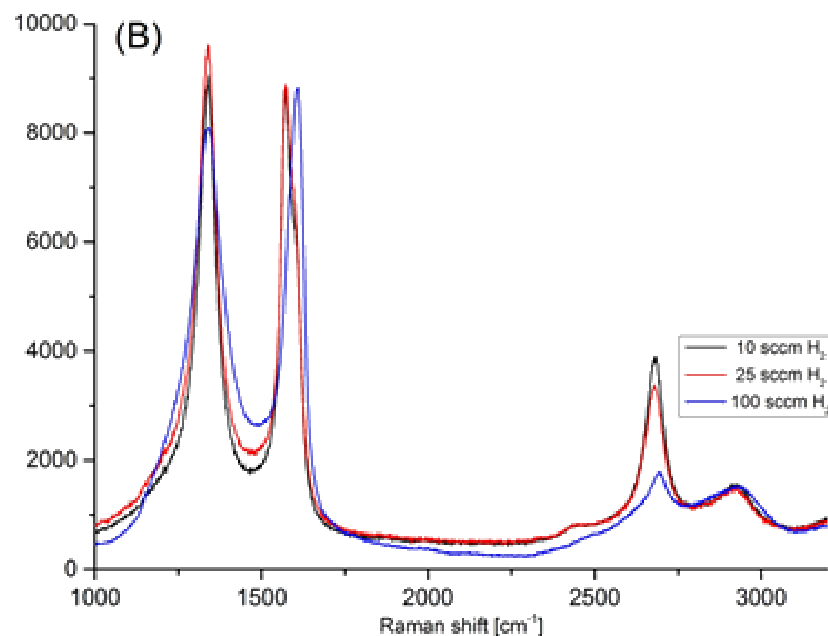

Influence of gas admixtures of O_2 and H_2 – The quality of produced nanosheets decreases and we can see increase of I_D/I_{2D} ratio. At the same time our spectra does not correspond to graphene oxide structure.

Graphene nanosheets synthesis in gas phase at atmospheric pressure

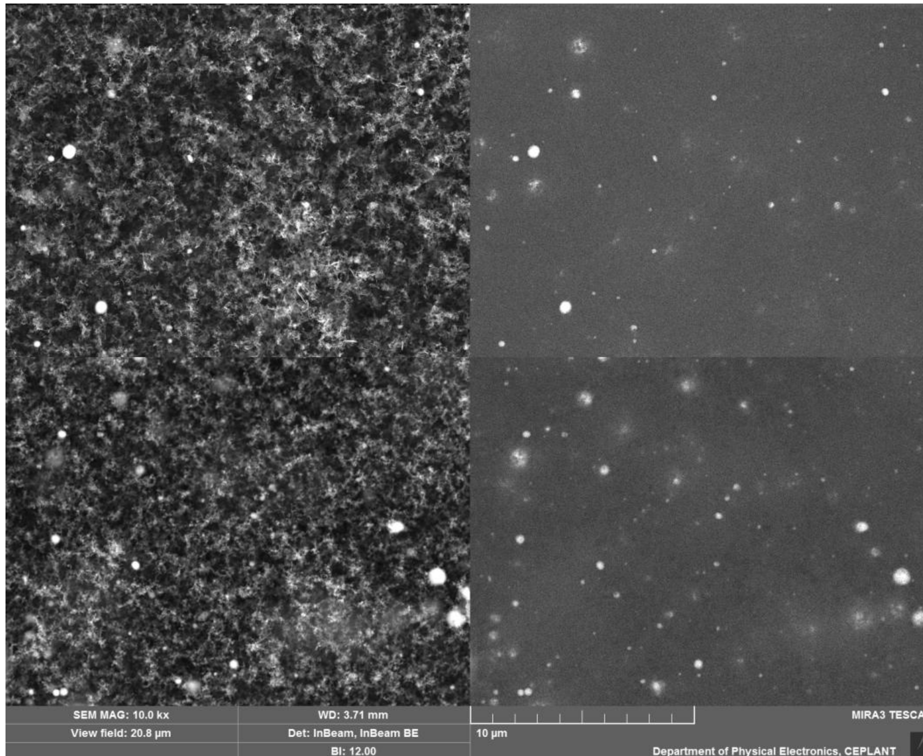

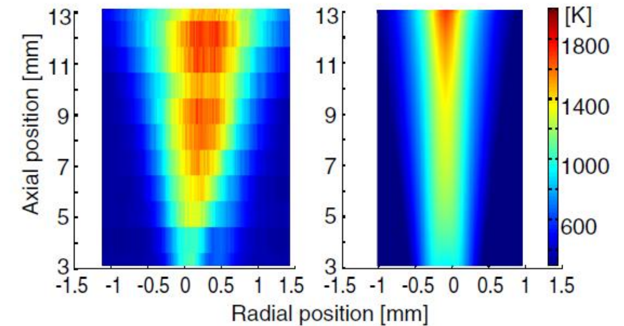

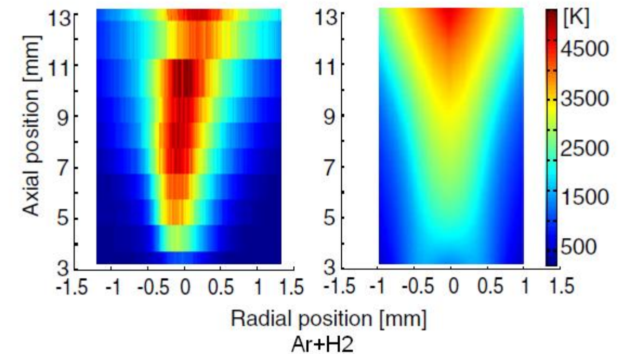

Iron particles contamination in hydrogen admixture mode

Plasma reduction of graphene oxide

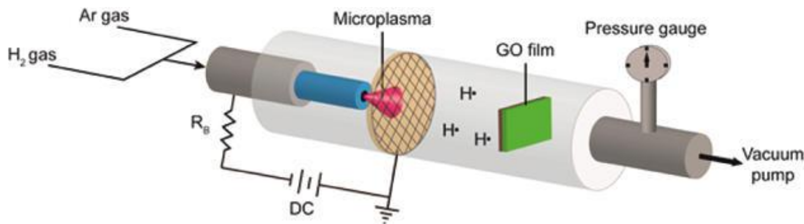

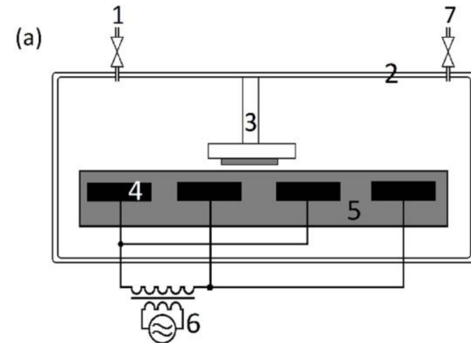

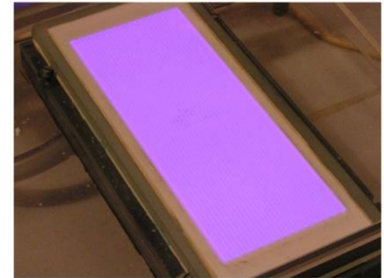

1 - Gas inlet, 2 - PMMA lid, 3 - Sample holder,
4 - Electrodes, 5 - Dielectric, 6 - Power supply,
7 - Gas outlet

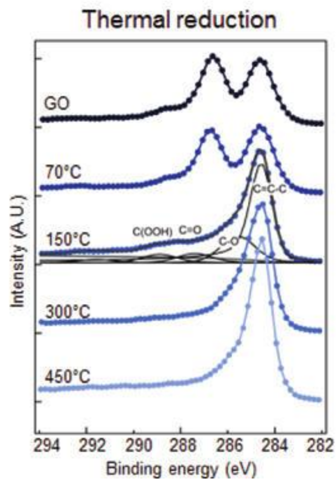

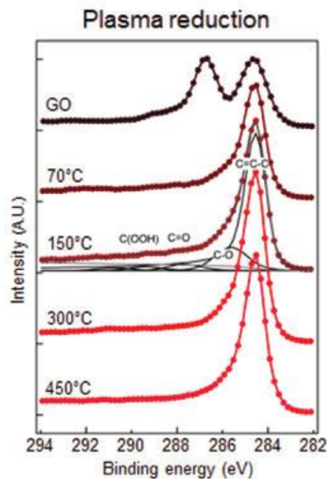

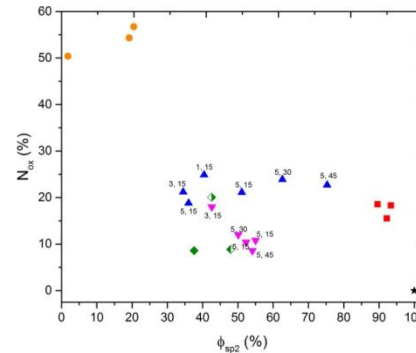

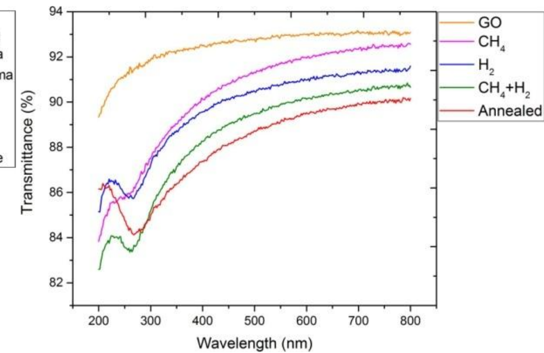

S.W. Lee et al., Plasma-Assisted Reduction of Graphene Oxide at Low Temperature and Atmospheric Pressure for Flexible Conductor Applications, J. Phys. Chem. Lett. 2012, 3, 772−777.
M.Bodik et al., Fast low-temperature plasma reduction of monolayer graphene oxide at atmospheric Pressure, Nanotechnology 28 (2017) 145601.

Graphene nanoribbons

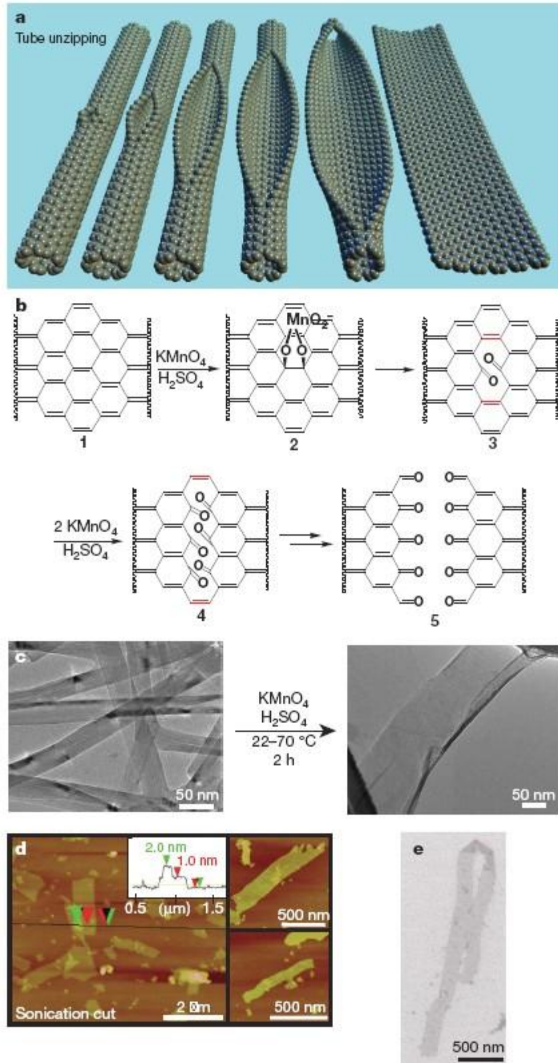

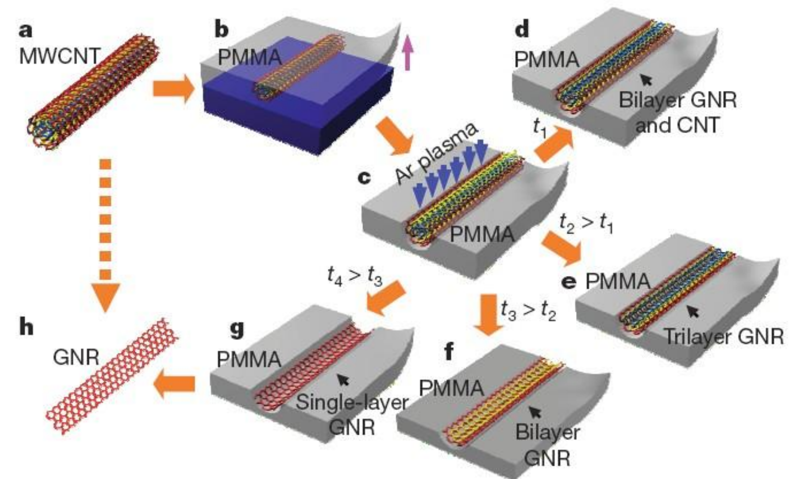

Figure 1 | Making GNRs from CNTs. **a**, A pristine MWCNT was used as the starting raw material. **b**, The MWCNT was deposited on a Si substrate and then coated with a PMMA film. **c**, The PMMA–MWCNT film was peeled from the Si substrate, turned over and then exposed to an Ar plasma. **d**–**g**, Several possible products were generated after etching for different times: GNRs with CNT cores were obtained after etching for a short time t_1 (**d**); tri-, bi- and single-layer GNRs were produced after etching for times t_2, t_3 and t_4, respectively ($t_4 > t_3 > t_2 > t_1$; **e**–**g**). **h**, The PMMA was removed to release the GNR.

Liying Jiao et al., Narrow graphene nanoribbons from carbon nanotubes, 458, Nature, 877.

Dmitry V. Kosynkin et al., Longitudinal unzipping of carbon nanotubes to form graphene nanoribbons, Nature, 458, 2009, 872.

P. Ruffieux et al., On-surface synthesis of graphene nanoribbons with zigzag edge topology, Nature, 531, 2016, 489.

GNR – zig-zag metallic, archmchair – metallic and semiconducting

Graphene transfer to dielectric substrate

- Graphene transfer scheme on Cu foil: a) PMMA mask b) etching of graphene on one side of the foil in O_2 plasma, c) chemical etching of Cu (for example in $FeCl_3$) d) transfer of PMMA+graphene to dielectric substrate e) chemical or plasma etching of PMMA.
- Gao, L. *et al. Nature* ***505, 190–194 (2014).***

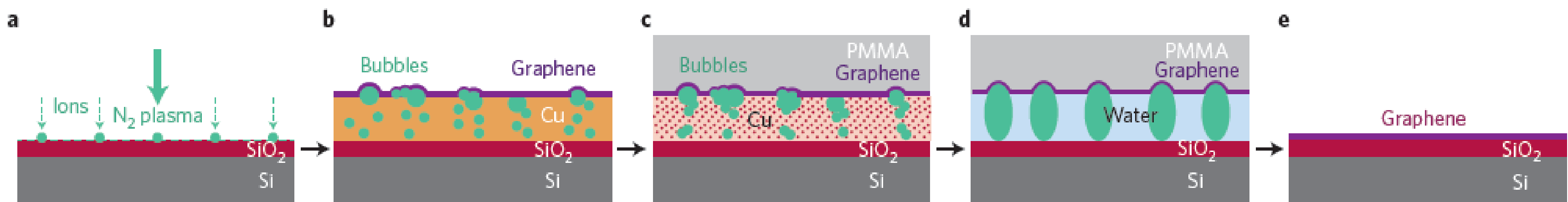

Literature

- M. Meyyappan, L. Delzeit, A. Cassell, D. Hash. *Plasma Sources Sci. Technol*. **12**, 205 (2003)
- M. Meyyappan, J. Phys. D: Appl. Phys. **42** (2009) 213001
- T. Nozaki, S. Yoshida, T. Karatsu and K. Okazaki, Atmospheric-pressure plasma synthesis of carbon nanotubes, J. Phys. D: Appl. Phys. 44 (2011) 174007 (9pp)
- Z. Bo et al., Plasma-enhanced chemical vapor deposition synthesis of vertically oriented graphene nanosheets, Nanoscale, 2013, 5, 5180.
- E. Tatarova et al. Microwave plasma based single step method for free standing graphene synthesis at atmospheric conditions. *Applied Physics Letters*, 2013, 103.13: 134101.
- X. Chen, B. Wu, Y. Liu, Direct preparation of high quality graphene on dielectric substrates, ***Chem. Soc. Rev., 2016,*** 45, 2057.
- Commercial presentations: AIXTRON Black Magic, Oxford Nanofab